

SOME FAST REACTIONS IN MIXED SOLVENTS

A Dissertation
Presented to the
Faculty of the Department of Chemistry
College of Arts and Sciences
University of Houston

In Partial Fulfillment
of the Requirements for the Degree
Doctor of Philosophy

by
Chin-tung Lin
May, 1970

558125

ACKNOWLEDGEMENTS

I am deeply indebted to my major professor, Dr. John L. Bear for his aid, patience and advice during the course of the study. I also wish to express my appreciation to Mr. Jack Harrell, Mr. S. Zubairi and especially, Dr. A. F. Hildebrandt for their many invaluable discussions and suggestions, to Mr. Robert Adams for his laboratory assistance, to Miss Linda Anderson and to my wife, Tammy, for their secretarial work in the preparation of the manuscript. Finally, I wish to thank the Welch Foundation for providing a predoctoral fellowship in support of this research.

SOME FAST REACTIONS IN MIXED SOLVENTS

An Abstract

Presented to the
Faculty of the Department of Chemistry
College of Arts and Sciences
University of Houston

In Partial Fulfillment
of the Requirements for the Degree
Doctor of Philosophy

by
Chin-tung Lin
May, 1970

ABSTRACT

The stability constants and the rate constants for the formation of the one-to-one complexes of nickel and several of the lanthanides with singly charged murexide in H_2O , 25% DMSO- H_2O , 50% DMSO- H_2O and 50% ethanol - H_2O mixed solvents have been determined at different temperatures. The formation constants were calculated from spectrophotometric data and the kinetic studies were made on a temperature jump apparatus. The thermodynamic and kinetic parameters obtained from these measurements for the nickel system are interpreted in terms of dielectric constant of the mixed solvents and intermolecular interactions in the solvents. The slowness of nickel murexide complexation reactions compared to other nickel systems reported in the literature is explained by the fast stepwise dissociation of metal-ligand bonds rather than by the chelate ring closure mechanism. After analysis of these data and some literature values for the lanthanide ligand substitution reactions, it is concluded that the process of eliminating the water molecule from the solvated metal ions is coupled to an outer sphere ion pair formation reaction and may be subject to a ligand effect.

TABLE OF CONTENTS

CHAPTER	PAGE
ACKNOWLEDGEMENTS.....	i
ABSTRACT	ii
I. INTRODUCTION.....	1
II. THEORY.....	8
1. The Relaxation Time and the Rate Constant.....	8
2. Diffusion-Controlled Reactions and Ion Association Equilibrium.....	14
3. The Relaxation Times for Coupled Reactions.....	17
4. The Chemical Application of Relaxation Functions.....	22
III. EXPERIMENTAL.....	28
1. Nature of the Temperature Jump Apparatus.....	28
2. Apparatus.....	31
3. Equilibrium Constant Measurements.....	36
a) Principle.....	36
b) Preparation of the Solutions.....	38
4. Kinetic Measurements.....	39
IV. RESULTS AND DISCUSSION.....	49
1. Thermodynamic Section.....	49
2. Kinetic Section.....	70
a) Nickel Murexide Complex Formation.....	70
b) Lanthanide Murexide Complex Formation.....	89
BIBLIOGRAPHY.....	101

LIST OF TABLES

TABLE	PAGE
I. Methods for Studying fast Reactions in Solution and Time Range Covered.	2
II. Ion Pair Constants at 25°C.	18
III. Characteristics of a Standard Temperature Jump Cell	30
IV. Rate Constants and λ_{\max} and ϵ_{\max} of some Indicators	40
V. Transmittance of Terbium(III) Murexide in 50% Ethanol Aqueous Solution as a Function of pH and Wavelength	55
VI. Molecular Extinction Coefficients of Metal Chelates and Perpureate Ion.	57
VII. Stability Constants for the 1:1 Nickel(II) Murexide in Aqueous Solution at $\lambda = 460 \text{ nm}$, Ionic Strength = 0.1 M and pH = 5.	58
VIII. Stability Constants for the 1:1 Nickel(II) Murexide in 50% DMSO Aqueous Solution at $\lambda = 460 \text{ nm}$, Ionic Strength = 0.1 M and pH = 5.3.	59
IX. Stability Constants for the 1:1 Nickel(II) Murexide in 25% Aqueous DMSO Solutions at $\lambda = 460 \text{ nm}$, Temperature = 25°C, Ionic Strength = 0.1 M and pH = 5	60
X. Stability Constants for the 1:1 Nickel(II) Murexide in 50% Ethanol Aqueous Solution at $\lambda = 460 \text{ nm}$, Temperature = 25°C, Ionic Strength = 0.1 M and pH = 5	61

LIST OF TABLES (continued)

TABLE	PAGE
XI. Stability Constants for the 1:1 Holmium(III) Murexide in 50% Aqueous Ethanol Solution at $\lambda = 470$ nm, Temperature = 12°C, Ionic Strength = 0.1 M and pH = 5 . .	62
XII. Stability Constants for the 1:1 Dysprosium(III) Murexide in 50% Aqueous Ethanol Solution at $\lambda = 470$ nm, Temperature = 12°C, Ionic Strength = 0.1 M and pH = 5	63
XIII. Stability Constant for the 1:1 Terbium(III) Murexide in 50% Aqueous Ethanol Solution at $\lambda = 470$ nm, Temperature = 12°C, Ionic Strength = 0.1 M and pH = 5	64
XIV. Stability Constant for the 1:1 Gadolinium(III) Murexide in 50% Aqueous Ethanol Solution at $\lambda = 470$ nm, Temperature = 12°C, Ionic Strength = 0.1 M and pH = 5	65
XV. Stability Constant for the 1:1 Samarium(III) Murexide in 50% Aqueous Ethanol Solution at $\lambda = 470$ nm, Temperature = 12°C, Ionic Strength = 0.1 M and pH = 5	66
XVI. Stability Constant for the 1:1 Europium(III) Murexide in 50% Aqueous Ethanol Solution at $\lambda = 470$ nm, Temperature = 12°C, Ionic Strength = 0.1 M and pH = 5	67
XVII. Selected Complexation Rate Constants for Cobalt(II) and Nickel(II).	76
XVIII. Relaxation Times and k_{1f} for Nickel(II) Murexide in Aqueous Solution at Ionic Strength = 0.1 M, pH = 5, and $\lambda_{\max} = 460$ nm	78

LIST OF TABLES (continued)

TABLE	PAGE
XIX. Kinetic Data for the Nickel(II) Murexide Formation at 20°C and Ionic Strength = 0.1 M.	83
XX. Solvent - Exchange Rate Parameters and Dq Values for Nickel(II) and Cobalt(II) Systems	85
XXI. Relaxation Times and k_{1f} for the Nickel(II) Murexide Formation in Various Solvent Systems, Ionic Strength = 0.1 M, pH ~ 5, $\lambda_{\max} = 460$ nm.	86
XXII. The k_{1f} and k_{1r} Values Extrapolated to 25°C for the Nickel(II) Murexide Formation in Various Solvent Systems at Ionic Strength = 0.1 M	88
XXIII. The Theoretical Ion Pair Constants (K_0) and Diffusion Controlled Rate Constants at 25°C	91
XXIV. Summary of Kinetic Data for the Lanthanide - Anthranilate and Murexide Systems.	93
XXV. Kinetic Data and Rates for the Lanthanide - Murexide Systems in 50% Ethanol - H ₂ O Solution at 12°C	97

LIST OF FIGURES

FIGURE	PAGE
1. Multiple Step Complex Formation Mechanism	4
2. Relaxation Response Following a Rectangular Step Function	10
3. Schematic Diagram of a Temperature Jump Apparatus	32
4. Schematic Diagram of a Photomultiplier and a Detection Circuit	34
5. Temperature Jump Oscillogram for an Aqueous $10^{-5}M$ Phenolphthalene in 0.1 M KNO_3 Solution with pH 9.2 at Room Temperature.	41
6. Temperature Jump Oscillogram for an Aqueous $6 \times 10^{-5}M$ Phenolphthalene in 0.1 M KNO_3 Solution with pH 9.2 at Room Temperature.	41
7. Experimental Relaxation Curve for Nickel(II) Murexide . .	43
8. Experimental Relaxation Curve for Nickel(II) Murexide . .	43
9. Experimental Relaxation Curve for Nickel(II) Murexide . .	44
10. Experimental Relaxation Curve for Nickel(II) Murexide . .	44
11. Experimental Relaxation Curve for Nickel(II) Murexide . .	45
12. Experimental Relaxation Curve for Nickel(II) Murexide . .	45
13. Experimental Relaxation Curve for Nickel(II) Murexide . .	46
14. Experimental Relaxation Curve for Terbium(II) Murexide. .	47
15. Experimental Relaxation Curve for Gadolinium(III) Murexide.	47
16. Experimental Relaxation Curve for Holmium(III) Murexide .	48

LIST OF FIGURES (continued)

FIGURE	PAGE
17. Experimental Relaxation Curve for Dysprosium(III) Murexide.	48
18. Absorption Spectra of Nickel(II) Murexide at Various pH's in Aqueous Solution.	52
19. Absorption Spectra of Nickel(II) Murexide at Various pH's in 25% DMSO Aqueous Solution	53
20. Absorption Spectra of Nickel(II) Murexide at Various pH's in 50% DMSO and 50% Ethanol Aqueous Solutions.	54

I

INTRODUCTION

INTRODUCTION

In order to study elementary steps in reaction mechanisms with each step involving only one transition state, techniques must be used which permit detection of reaction intermediates and permit kinetic studies in a very wide time range. This may encompass times from as short as molecular physical motions (about 10^{-13} sec.⁻¹) to as long as the reaction requires. New techniques for the investigation of very rapid reactions in solution have become available only in recent years. Some of the new methods for studying very fast reactions in solution and the time range covered are shown in Table I (1). Several of the techniques listed in Table I are relaxation methods and deal only with rate phenomena that take place near equilibrium. Relaxation methods are quite simple in concept. The reaction whose rate is to be studied reaches a position of equilibrium determined by a set of external parameters such as temperature and pressure. If a change in one of these parameters is made suddenly, there is a finite time lag while the system approaches the new position of equilibrium governed by the new set of external parameters. This time lag is related to the rate constants of the forward and reverse reaction. The course of the reaction may be followed by various means such as the spectrophotometer for the temperature jump method (2) and the conductivity bridge for the pressure jump method (3,4).

Most of the experimental data on rates of metal ligand substitution reactions in aqueous solution can be explained by two

TABLE I
METHODS FOR STUDYING FAST REACTIONS
IN SOLUTION AND TIME RANGE COVERED

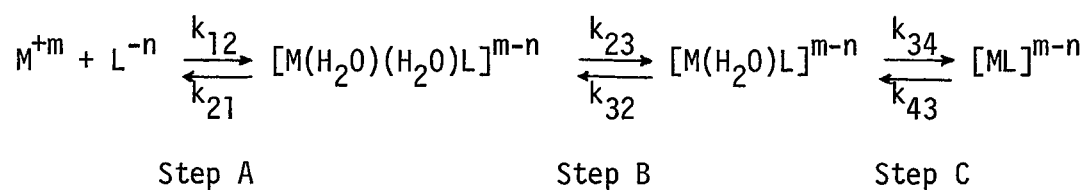
Method	Time Range (sec)
Flow	10^{-3} — 1
Temperature jump	10^{-6} — 1
Pressure jump	10^{-5} — 1
Electric field jump	10^{-8} — 10^{-4}
Ultrasonic	10^{-10} — 10^{-5}
Nuclear magnetic resonance	10^{-7} — 1
Flash photolysis	10^{-6} — 1
Electrochemical	10^{-4} — 1

mechanisms (5). For one of these mechanisms, the rate determining step of complex formation is either strongly dependent on the nature of the metal ion or is sterically controlled by the entering ligand (6,6'). Systematic studies have shown that the divalent ions of the first transition series and the alkaline earth series react by this mechanism. The first mechanism is a multiple step mechanism and is shown in Figure 1. This mechanism was proposed by Eigen (7-9) and coworkers and will be discussed later. Ions which show strong hydrolyzes readily, such as Fe^{+3} and Be^{+2} , react by the second mechanism. For these ions, the rate is strongly dependent on the basicity of the entering ligand. The distinguishing characteristics of this group is that the rate of hydrolysis exceeds appreciably the possible rate of substitution in the unhydrolyzed complex.

For the reaction between H^+ and OH^- ions, the results indicate that the proton can be transferred without hindrance along a symmetrical hydrogen bond (12). This leads to the conclusion that protolytic reactions in general may be diffusion controlled as long as the proton is bound more tightly at the proton acceptor than at the donor. Intramolecular hydrogen bonding at the reaction site will slow down the rate of acid-base reactions, since a proton involved in an internal hydrogen bond is not available for reaction unless the internal H-bond is broken and bridging with the water structure takes place. A good example of this occurs in N,N-dimethyl-o-amino benzoic acid (11) where the rate of reaction with an hydroxide is about 3 orders of magnitude below "normal

FIGURE 1

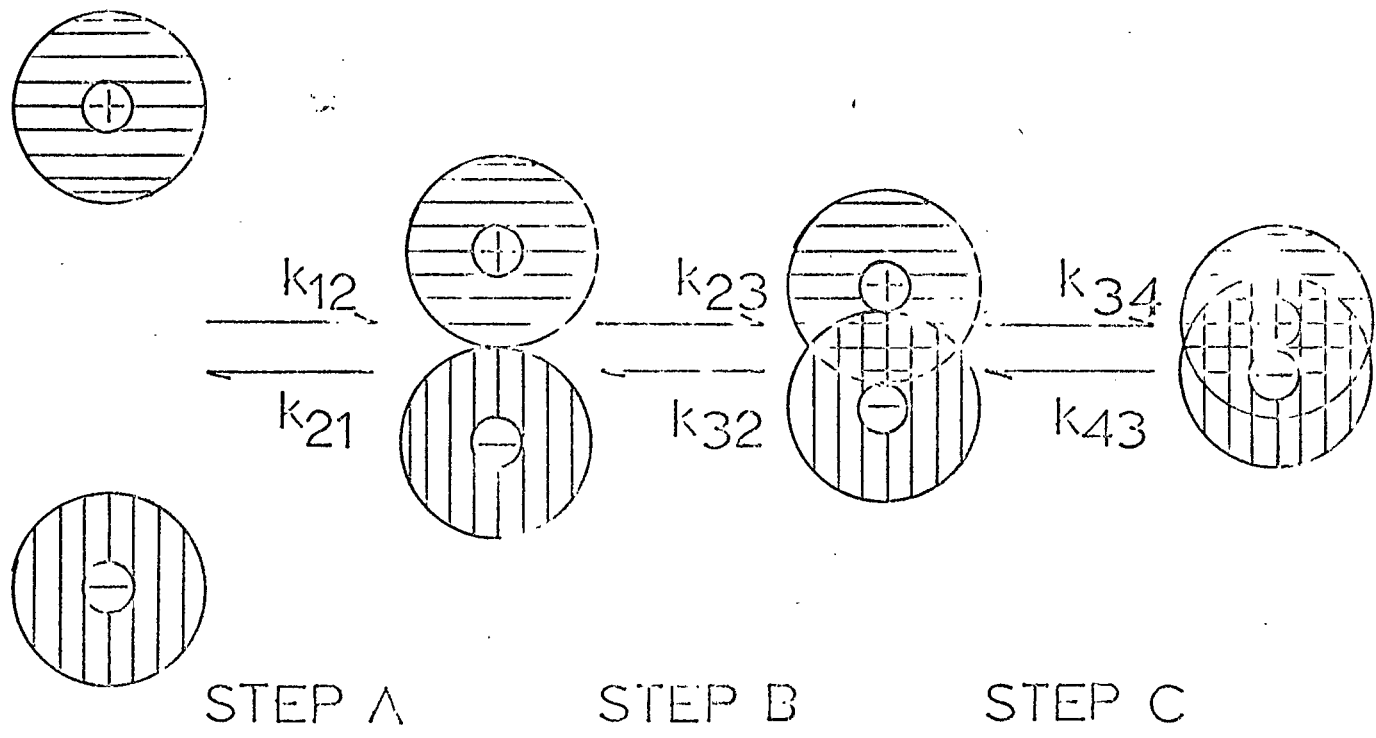
MULTIPLE STEP COMPLEX FORMATION MECHANISM



Step A = Formation of Bjerrum Ion Pair

Step B = Formation of Outer Sphere Coordination Complex

Step C = Formation of Inner Sphere Coordination Complex



rates". The acid association constant of this compound is thus reduced by the same order of magnitude compared to that of the parent acid. The relaxation time associated with reactions in pure water has been measured and the rate constant for the neutralization reaction is $1.4 \times 10^{11} \text{ M}^{-1} \text{ sec.}^{-1}$ (10). Using this constant, the "reaction distance" or the distance of closest approach of a proton to a hydroxyl ion before the two react has been calculated to be 8 \AA . This value demonstrates that the proton and the hydroxyl ion exist in water principally not as the simple ions, H_3O^+ and OH^- , but as the complexes, H_9O_4^+ and H_7O_4^- , which have diameters of about 8 \AA .

In recent years, fast reaction studies have been extended to mixed solvent and nonaqueous solvent systems (13-17). From these studies it has been concluded that the rate of solvent exchange between the coordination sphere of metal ions and the bulk solvent depends upon: (1) metal--ligand bond energies, (2) solvation difference between ground and transition states, (3) steric requirements of the different ligands, and (4) the ability of the ligands to provide electronic stabilization for a state of reduced coordination number (17). Basolo and Pearson (18) have proposed that the relative exchange rates may be explained only by the differences in loss of crystal field stabilization on going from the octahedral complex to the transition state. This theory predicts qualitatively that the activation enthalpy, ΔH^* , for exchange should parallel the crystal field splitting parameter Dq . However, it has been found that the qualitative predictions of this

theory are not in agreement with the experimental results of fast reactions studied in various nonaqueous solutions (16). This is because the consideration of reactant and transition state solvation has long been neglected. In another study by a pressure jump technique (19) in this laboratory, it was found that the difference in the rate of ligand substitution reactions between magnesium and other alkaline earth ions can best be explained by differences in solvation between the ground and transition states.

The kinetics of complexation of cobalt(II) and nickel(II) with the oligoglycine (Diglycine, triglycine and tetraglycine) have been reported in the literature (20,21). The reaction with cobalt(II) is normal, while that with nickel(II) is inhibited compared to the rates with other ligands. The possibility of the sterically hindered chelate ring closure being the rate-determining step is excluded, since the experimental results show that the effect was exhibited by ions more labile than nickel(II), namely, cobalt(II) and manganese(II) but not by nickel(II) itself (6,22). Therefore it has been suggested that the bonding model is somewhat different for the nickel complexes of these oligopeptides than for cobalt(II) complexes (21,23).

In light of the above discussion and the fact that similar observations have been found between these two metal ions and murexide in aqueous solution (24), the kinetics and thermodynamics of nickel(II) murexide complexation in H_2O , ethanol- H_2O , and DMSO- H_2O solutions were studied independently by using the temperature jump apparatus and the spectrophotometry, respectively.

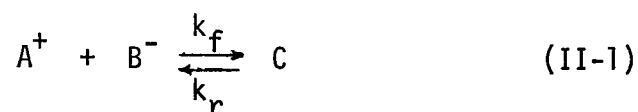
As far as the solution chemistry of the trivalent lanthanide ions is concerned, the unusual variations in stability noted for complexes of these ions have been the major interest in the study of this type of complexation reaction (25). Recently, kinetic studies of several lanthanide systems in aqueous solution have been carried out using relaxation techniques (24,26-29). Unexpectedly, no similarities have been found for these systems as those observed previously for divalent transition metal ions. The rates of lanthanide reactions reported do not seem to correspond to one another if the same mechanism is assumed. The present studies are aimed at elucidating some of these differences on the basis of literature values and the rate constants obtained for the lanthanide murexide formation reactions in ethanol-H₂O mixed solvents.

II
THEORY

THEORY

1. The Relaxation Time and the Rate Constant

A simplified one-step equilibrium such as complex formation or ion association that is experimentally encountered, can be written as follows (30):



If the system is initially at equilibrium for the species, A^+ , B^- , and C , respectively, when the equilibrium conditions are suddenly disturbed, the reaction will be shifted to a new equilibrium where the equilibrium concentrations are now \bar{C}_a , \bar{C}_b , and \bar{C}_c . At time t , the actual concentrations (C_a , C_b , C_c) differ from these by an amount x , so that,

$$x = C_a - \bar{C}_a = C_b - \bar{C}_b = \bar{C}_c - C_c. \quad (\text{II-2})$$

The net forward rate at time t is given by

$$-\frac{dx}{dt} = k_f C_a C_b - k_r C_c \quad (\text{II-3})$$

which at equilibrium becomes

$$k_f \bar{C}_a \bar{C}_b - k_r \bar{C}_c = 0. \quad (\text{II-4})$$

The net forward rate is obtained in terms of x by substituting $C_a = \bar{C}_a + x$, $C_b = \bar{C}_b + x$ and $C_c = \bar{C}_c - x$ into equation (II-3). From equation (II-4), the following relationship is obtained by assuming only a small displacement for the reaction.

$$-\frac{dx}{dt} = [k_f(\bar{C}_a + \bar{C}_b) + k_r]x \quad (\text{II-5})$$

The quantity in brackets is a constant, independent of time. Integration of equation (II-5) gives

$$\frac{x}{x_0} = e^{-[k_f(\bar{C}_a + \bar{C}_b) + k_r]t} \quad (\text{II-6})$$

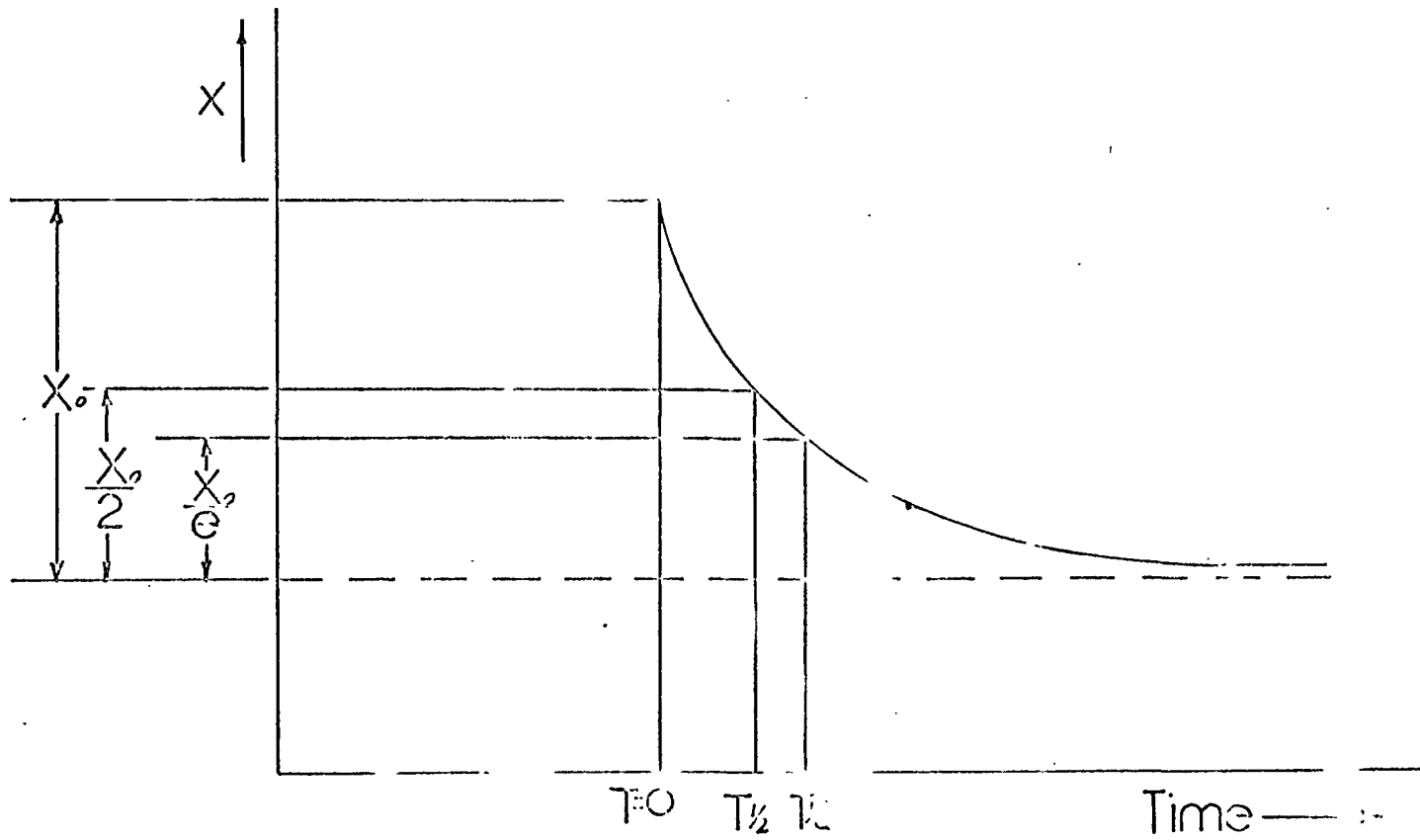
where x_0 is the value of x immediately after the disturbance. Equation (II-6) describes the course of equilibration which is illustrated in Figure 2. It implies that after a time interval such that $[k_f(\bar{C}_a + \bar{C}_b) + k_r]t = 1$, then $\frac{x}{x_0} = \frac{1}{e}$; that is, the difference between the actual concentrations and equilibrium concentrations has been reduced to $\frac{1}{e}$ of the original difference. It is convenient to define this time interval as the relaxation time, denoted by τ . The relaxation time at a series of concentrations can be found experimentally. Therefore, a plot of $\frac{1}{\tau}$ against $(\bar{C}_a + \bar{C}_b)$ yields a straight line where the slope is the forward rate constant and the intercept is the reverse rate constant as shown below.

$$\tau^{-1} = k_f(\bar{C}_a + \bar{C}_b) + k_r = k_f^{\circ} \gamma_{\pm}^2 (\bar{C}_a + \bar{C}_b) + k_r \quad (\text{II-7})$$

FIGURE 2

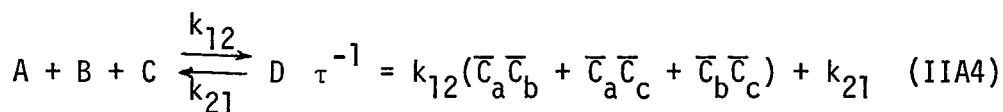
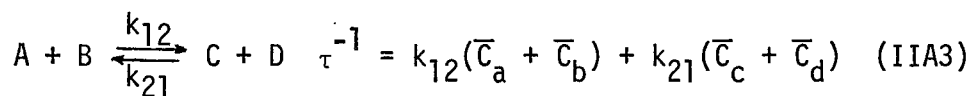
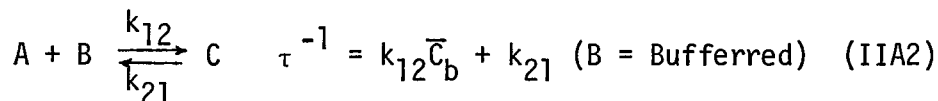
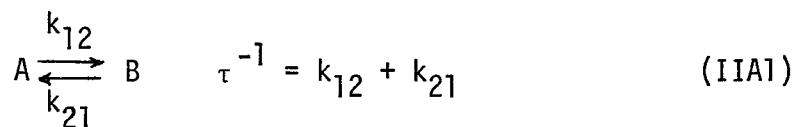
RELAXATION RESPONSE FOLLOWING
A RECTANGULAR STEP FUNCTION

$T_{\frac{1}{e}} = \tau =$ Relaxation time for a
single step reaction



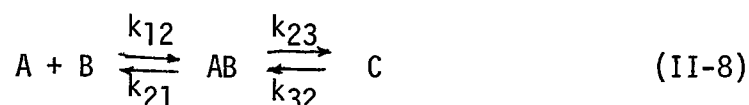
where k_f° is the rate constant at zero ionic strength and γ_{\pm} is the mean activity coefficient.

The relationship between the relaxation times and the rate constants for the following reaction system can be derived by a similar procedure as follows (31):



For ionic reactions, Eigen and his associates (31) have shown that the rate constants usually include concentration dependent terms, as a result of electrostatic interactions with other ions present in the system. The ionic interactions can be described in terms of activity coefficients, which occurs in k_f , where k_r remains concentration independent as shown in equation (II-7).

In a reaction system,



The rate equations for a small displacement can be written by the procedure previously described (32)

$$-\frac{dx_1}{dt} = \{k_{12}(\bar{c}_a + \bar{c}_b) + k_{21}\} x_1 + k_{21}x_3 = a_{11}x_1 + a_{12}x_3 \quad (\text{II-9})$$

$$-\frac{dx_3}{dt} = k_{23}x_1 + (k_{32} + k_{23})x_3 = a_{21}x_1 + a_{22}x_3 \quad (\text{II-10})$$

with

$$x_1 = c_a - \bar{c}_a = c_b - \bar{c}_b; \quad x_2 = c_{ab} - \bar{c}_{ab}; \quad x_3 = c_c - \bar{c}_c$$

$$\text{and } x_1 + x_2 + x_3 = 0$$

The solutions of relaxation times for the above mechanism are given by

$$\frac{1}{\tau} = \frac{1}{2} \left\{ (a_{11} + a_{22}) \pm \sqrt{(a_{11} + a_{22})^2 - 4(a_{12}a_{21} - a_{11}a_{22})} \right\} \quad (\text{II-11a})$$

or

$$\frac{1}{\tau} = \frac{1}{2} \left\{ k_{12}[\bar{c}_a + \bar{c}_b] + k_{21} + k_{23} + k_{32} \right\} \left\{ 1 \pm \sqrt{1 - 4 \frac{k_{12}k_{23}[\bar{c}_a + \bar{c}_b] + k_{12}k_{32}[\bar{c}_a + \bar{c}_b] + k_{21}k_{32}}{[k_{12}(\bar{c}_a + \bar{c}_b) + k_{21} + k_{23} + k_{32}]^2}} \right\} \quad (\text{II-11b})$$

With the assumption that the bimolecular step is very fast compared to the unimolecular step; that is, $k_{12}[\bar{c}_a + \bar{c}_b] + k_{21} \gg k_{32} + k_{23}$. The results are

$$\begin{aligned}\frac{1}{\tau_1} &= k_{12}[\bar{C}_a + \bar{C}_b] + k_{21} \\ &= k_{12}f(C) + k_{21}\end{aligned}\quad (\text{II-12})$$

$$\frac{1}{\tau_2} = \frac{K_a f(C)}{1 + K_a f(C)} k_{23} + k_{32} \quad (\text{II-13})$$

where K_a is equal to $\frac{k_{12}}{k_{21}}$,

where τ_1 and τ_2 refer to the relaxation times corresponding to step I and step II respectively.

A generalized equation thus can be derived for the mechanism, as shown in Figure I, in which

$$\frac{1}{\tau_i} = k_{k1}''[f(C)] + k_{1k} \quad (\text{II-14})$$

where k_{k1} are the effective rate constants defined specifically by:

$$k_{12}'' = k_{12} \quad (\text{II-15})$$

$$k_{23}'' = \frac{K_a}{1 + K_a[f(C)]} k_{23} \quad (\text{II-16})$$

$$k_{34}'' = \frac{K_a K_b}{1 + K_a(1 + K_b)[f(C)]} k_{34} \quad (\text{II-17})$$

K_a and K_b are stability constants for step a and b respectively, and k_{34} , k_{43} are much smaller than k_{12} , k_{21} or k_{23} , k_{32} .

The above treatment shows that the observed rate constants for each step not only depend on the ionic interactions but also on concentrations of the free ions and the stability constants for the ion pair formation. Thus, only in very dilute solutions and with complexes with a small stability constant can k_{k1} be treated as a constant. Otherwise, the plot of concentrations of the free ions against the reciprocal of the relaxation times will not give a straight line.

2. Diffusion-Controlled Reactions and Ion Association Equilibrium.

The theory for diffusion-controlled reactions was first developed by Smoluchowski (33). The theory was derived assuming that the diffusive motions of molecules can be treated like the motions of macroscopic spherical particles in a viscous fluid. Considering a solution having two types of solute molecules A and B with equal molecular radii, a simple expression has been obtained as follows:

$$k_D = \frac{8RT}{3000\eta} \quad 1 \text{ mole}^{-1} \text{ sec}^{-1} \quad (\text{II-18})$$

This equation predicts that the rate constant of a diffusion-controlled reaction will be inversely proportional to the viscosity (η). It has been shown that reaction rates will generally not be affected within one percent by the rate of diffusion if the rate constant is less than $10^7 \text{ l mole}^{-1} \text{ sec}^{-1}$ (34,35). The theory was extended by Debye (36) to ionic solutions where long-range electrostatic forces were taken into account.

$$k_D = \left(\frac{8RT}{3000\eta} \right) \cdot \left(\frac{\delta}{e^{\delta} - 1} \right) \quad (\text{II-19})$$

$$\delta = \frac{Z_A Z_B e^2}{DkTa} \quad (\text{II-20})$$

Here Z_A and Z_B are the charge on the ions, e , the electronic charge, D , the dielectric constant, k , the Boltzmann's constant, and, a , the distance of closest approach of the ions. For reactions of oppositely-charged univalent ions in aqueous solution, k_D is between 10^{10} and 10^{11} $\text{l mol}^{-1} \text{sec.}^{-1}$ at room temperature with "a" between 1 \AA and 10 \AA .

It has been suggested that the rate of formation of an outer sphere complex, as shown in Figure 1, is close to diffusion controlled ion pair formation (31). The ion pair constant (K_o) for the reaction type, as shown in equation (II-21), has been derived independently by Fuoss (37) on statistical and by Eigen (38) on kinetic grounds,



$$K_o = \frac{\bar{C}_{ab}}{\bar{C}_a \bar{C}_b} = K_o^o e^{-b/\gamma_{\pm}^2} \quad (\text{II-22})$$

where

$$K_o^o = \frac{4\pi Na^3}{3000} \quad (\text{II-23})$$

$$b = \left| Z_A Z_B \right| e^2 / DkTa \quad (\text{II-24})$$

$$\gamma_{\pm}^2 = \exp[-bk'a/(1+k'a)] \quad (\text{II-25})$$

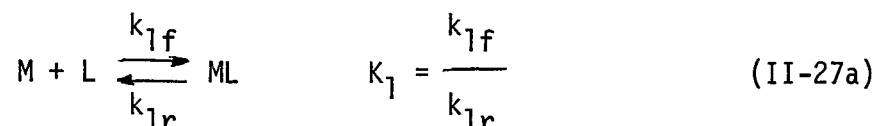
$$k' = \frac{8\pi N e^2}{1000 DKT} \mu \quad (\text{II-26})$$

In the above equations, K_0^0 is the association constant for uncharged particles, the term e^b is the ratio of the electrostatic energy to the thermal energy, $K_0^0 e^b$ is the association constant for charged particles at infinite dilution, r_{\pm}^2 is the square of the Debye-Hückel mean activity coefficient, N is Avogadro's number, μ is the ionic strength, and the rest of the symbols have the usual significance. Equation (II-22) has been based on models in which the solvent is assumed to be a continuum, the ions are considered to be rigid spheres of radii $a/2$, and the preexponential factor is entropic in nature (22). It increases with increasing ionic radius, reflecting the enhanced probability of pairing as the reaction cross section increases. The exponential factor is the energy part and is controlled mainly by the electrostatic interaction. This factor decreases with increasing ionic size. The value of K_0 calculated from the theoretical derivation is thought to be within a factor of 3 or 4 of the experimental value. However, for some ion pair formation reaction, a difference of two orders of magnitude has been found between the theoretical calculation and experimental value (39). Unfortunately, it is very difficult to obtain K_0 experimentally and an assumption of the value for K_0 must be made before the rate constant can be obtained for the metal-ligand substitution reactions studied by either the pressure-jump or the

ultrasonic technique. Therefore, one should be cautious in interpreting the results obtained by different techniques under different conditions and assumptions. A typical set of K_0 values computed from Equation (II-22) for methanol and water solutions at various ionic strength is shown in Table II (13).

3. The Relaxation Times for Coupled Reactions

For a metal-ligand complex formation reaction of the type



the expression for the relaxation time for the above reaction is shown in Equation (II-7). If the extent of reaction is followed by an indicator, In, and the ligand has ionizable groups, the appropriate protolytic equilibria must be included in the reaction mechanism,



If these protolytic reactions approach equilibrium much faster than the metal complex reactions, they can be assumed to be at equilibrium at all times. The relaxation time (τ_1) has been derived by Hammes and Stenifeld (20) from the rate law and mass conservation relationships as:

TABLE II
ION PAIR CONSTANTS AT 25°C

μ	$(Z_A = 2, Z_B = -1)$	$(Z_A = 2, Z_B = -2)$
	Methanol ($a = 6 \text{ \AA}$)	
0.50	3.3	20
0.30	4.6	40
0.10	10	130
0.05	16	500
0.00	170	50,000
	Water ($a = 5 \text{ \AA}$)	
0.50	1.2	4.5
0.30	1.4	.5
0.10	2.0	14
0.05	2.5	21
0.00	5.6	100

$$-\frac{dX_M}{dt} = \left\{ k_{1f} \left(\frac{\bar{M}}{1+\alpha'} + \bar{I} \right) + k_{1r} \right\} X_M$$

$$\frac{1}{\tau_1} = k_{1f} \left[\frac{\bar{M}}{1+\alpha'} + \bar{I} \right] + k_{1r} \quad (\text{II-28})$$

where

$$\alpha' = \frac{X_{ML}}{X_L} = \frac{\bar{H}^+}{K_L + \bar{I} \left[\frac{K_I + \bar{H}^+}{K_I + \bar{H}^+ + \bar{I}_n} \right]}$$

and α' is derived from

$$K_L [X_{HL}] = [\bar{H}^+] X_L + \bar{I} [X_{H^+}]$$

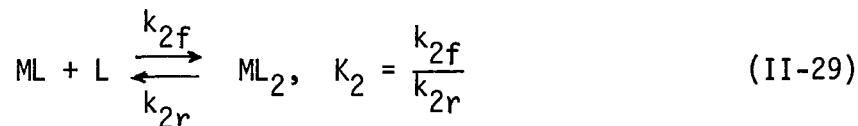
$$K_I [X_{H^+I_n}] = \bar{I}_n [X_{H^+}] + \bar{H}^+ [X_{I_n}]$$

$$- X_{HI_n} = X_{I_n}$$

$$X_{H^+L} + X_{H^+I_n} + X_{H^+} = 0$$

Here X represents the deviation from equilibrium of the variable under consideration, and K_L and K_I are the ionization constants for the ligand and indicator, respectively. The concentrations designated with a bar are the various concentrations at equilibrium, and the constant, α' , varies with the conditions of the experiment.

If there is a biscomplex reaction, in addition to reaction (II-27), the following reactions must be included.



The two relaxation times for the coupled processes of (II-27) and (II-29) are identical to the general expressions shown in Equation (II-11a). The procedure is to set up the rate equations for these reactions, and then solve for the relaxation times as shown in Equation (II-11a). The values for the a's are as follows.

$$a_{11} = k_{1r} + k_{1f} \left[\bar{L} + \frac{\bar{M}}{1+\alpha} \right]$$

$$a_{12} = k_{1r} - k_{1f} \left[\frac{\bar{M}}{1+\alpha} \right]$$

$$a_{21} = k_{2f} \left[\bar{L} - \frac{\bar{ML}}{1+\alpha} \right]$$

$$a_{22} = k_{2r} + k_{2f} \left[\bar{L} + \frac{\bar{ML}}{1+\alpha} \right]$$

Theoretically, two relaxation times for the above reactions should be observed if the proposed mechanism is correct. Usually, however, only the faster effect (positive root) can be seen (6). In order to obtain the four rate constants from the single observed relaxation time, a trial and error method must be employed. An adopted

set of trial rate constants, with $K_1 = \frac{k_{1f}}{k_{1r}}$ and $K_2 = \frac{k_{2f}}{k_{2r}}$, should yield uniformly good agreement between the relaxation times calculated from the trial rate constants and those obtained experimentally. It is obvious that it is usually impossible to determine the number of elementary reactions from the number of relaxation times observed. However, the number of relaxation times observed cannot be less than the number of elementary steps suggested for the reaction. The theoretical expressions for relaxation times are a function of the mechanism proposed, the experimental conditions, and the specific assumptions made. The derivation of the equations must, therefore, meet all these requirements. For example, Equation (II-13) should not be used if $k_{12}[\bar{C}_a + \bar{C}_b] + k_{21} \approx k_{32} + k_{23}$ or the Equation (II-7) must not be employed if the reaction (II-1) is coupled by a biscomplex reaction.

The resolution of relaxation spectrum will become extremely difficult if it contains several relaxation times having the same order of magnitude. For a single relaxation time, we have

$$D = D_0 e^{-t/\tau}$$

where D is the difference between the signal at $t=t$ and $t=\infty$. Therefore, a plot of $\log D$ versus t should be a straight line with a slope of $\frac{-1}{2.3\tau}$. The linearity of the plot attests to the validity of the assumption of a single relaxation process. The simplest way to get the relaxation time after it has been shown to be a single relaxation process is to evaluate the τ at the point where D is equal to $\frac{1}{e}D_0$ as shown in Figure 2.

The signal amplitude, D , is in general given by (20)

$$D = \sum_i^n D_{i0} e^{-t/\tau_i}$$

A plot of $\log D$ versus t will be a curve if $i > 1$. In practice, if the relaxation times differ by at least a factor of two at sufficiently long times, all of the terms of the series except that characterized by the longest relaxation time, say the n^{th} , will go to zero. Thus, a straight line can be drawn through the curve at long time intervals and the slope, $\frac{-1}{2.3\tau_n}$ and D_{n0} , determined. The term, $D_{n0} e^{-t/\tau_n}$, can now be subtracted from the series so that the resultant series becomes:

$$D' = D - D_{n0} e^{-t/\tau_n} = \sum_i^{n-1} D_{i0} e^{-t/\tau_i}$$

Repetition of this procedure will yield the n relaxation times.

4. The Chemical Application of Relaxation Functions

Consider a simple one step complex formation reaction:



If it is assumed that species C absorbs light in the visible or near ultraviolet region and the other species are transparent, then the relationship between concentration and light intensity, I , transmitted through the solution is

$$I = I_0 e^{-\epsilon_i C_i l} \quad (\text{II-30})$$

where ϵ_j is the molar extinction coefficient of the species C, l is the path length of the observation cell in cm, C_j is the concentration in moles/liter for C, and I_0 is the light intensity before passage through the cell. For a small concentration change, X_j in C_j ,

$$I + \delta I = I_0 e^{-\epsilon_j (C_j + X_j) l} = I_0 e^{-\epsilon_j C_j l} (1 - \epsilon_j l X_j)$$

or
$$\delta I = -\epsilon_j l I X_j \quad (\text{II-31})$$

Equation (II-6) has already shown that

$$X_j = X_{j0} e^{-t/\tau}$$

where X_j and X_{j0} have the usual meaning. Since the change in light intensity is directly proportional to the concentration change, the trace of change in light intensity obtained by absorption spectrophotometry is also a relaxation process with a relaxation time the same as for the chemical reaction. For a process having more than two relaxation times the physical meaning of τ_j should be redefined before a correlation between concentration change and light intensity change can be made. The following general method used originally by Eigen and Maeyer (31) will be reviewed. If the concentration change brought about by the change of an external parameter is very small with respect to the various equilibrium concentrations, then the rate that the system reequilibrates after perturbation is proportional to the time-dependent concentration change itself.

In terms of a rate law, Reaction (II-1) can be expressed as

$$-\frac{dx}{dt} = a'X \quad (\text{II-32})$$

Where X is the magnitude of the concentration change as usual, a' is a proportional constant as shown in Equation (II-5). It has already been shown that a' is the reciprocal of relaxation time ($\frac{1}{\tau}$).

If multiple relaxation processes are involved, the temporal change in the concentration of a reactant, $\frac{dx_i}{dt}$, may depend on all the concentrations of other reactants present. Therefore, we have the form

$$-\frac{dx_i}{dt} = \sum_j a_{ij} X_j.$$

where a_{ij} can be obtained from the coefficient of X_j in the rate equations. These coefficients contain rate constants and equilibrium concentrations as shown in Equation (II-9) and (II-10). There will be n equations if n independent variables (X_i) are present. If X_i is transformed into a set of new variables (y_i) such that each of the new variables can be written in the form of Equation (II-32), that is,

$$-\frac{dy_i}{dt} = b_{ii} y_i \quad (\text{II-33})$$

then y_i can be obtained by a coordinate transformation which is a linear combination of the true concentration variables (X_i).

$$Y_i = \sum_j M_{ij} X_j \quad (\text{II-33a})$$

$$X_i = \sum_j F_{ij} Y_j \quad (\text{II-33b})$$

In order to obtain the relaxation times ($\frac{1}{b_{ij}}$) for the hypothetical concentrations (y_i) as defined for single step reaction, the b_{ij} can be treated as the eigenvalue of the characteristic equation, which, in determinant form, reads

$$\begin{vmatrix} (a_{11} - b) & a_{12} & \dots & \dots & \dots & a_{1n} \\ a_{21} & (a_{22} - b) & & & & \\ \cdot & \cdot & \cdot & \cdot & \cdot & \cdot \\ \cdot & \cdot & \cdot & \cdot & \cdot & \cdot \\ \cdot & \cdot & \cdot & \cdot & \cdot & \cdot \\ \cdot & \cdot & \cdot & \cdot & \cdot & \cdot \\ a_{n1} & \dots & \dots & \dots & \dots & (a_{nn} - b) \end{vmatrix} = 0$$

Since a_{ij} 's are known from the rate law, the reciprocal of relaxation times for equation (II-33) can be obtained from the roots of $b(\frac{1}{\tau_i} = b_{ij})$. If matrices A, B and M are used to express the coefficients a_{ij} , b_{ij} and m_{ij} , respectively, then it can be found that $B = MAM^{-1}$ exists. Here M^{-1} is the inverse to the transformation matrix M. As soon as the m_{ij} has been obtained from the above relationship, F_{ij} can be calculated from the equations of the form (II-33a).

Equation (II-33b) can then be written as

$$\begin{aligned} X_i &= \sum_j F_{ij} Y_j = \sum_j F_{ij} Y_{j0} e^{-t/\tau_j} \\ &= \sum_j P_{ij} e^{-t/\tau_j} \end{aligned} \quad (\text{II-34})$$

where

$$Y_{io} = \sum_j m_{ij} X_{jo}, \quad P_{ij} = F_{ij} Y_{jo}$$

If X_i is the only absorbing species, then Equation (II-31) can be substituted into Equation (II-34)

$$\delta I = \sum_j \delta_{ij} e^{-t/\tau_j} \quad (\text{II-35})$$

with

$$\delta_{ij} = (-\epsilon_i \ell I) P_{ij}$$

Again, it is easily seen from Equation (II-35) that the various τ_j 's can be obtained from the experimental trace of the change in light intensity by using the method illustrated in Section C. If two or more species are light-absorbing, the principle can be extended similarly. Finally, the rate constants for the proposed mechanism can be evaluated from the value of τ_j 's.

As an example, considering a simple coupled reaction,



If L is the only light absorbing species, then Equation (II-34) can be simplified as

$$X_L = P_{\ell 1} e^{-t/\tau_1} + P_{\ell 2} e^{-t/\tau_2}$$

Since there are two mass balance equations with respect to M and L contained in the above coupled reactions, only two independent variables or concentrations (X_j) are involved in the reaction system. Theoretically in this system two relaxation times can be obtained. Experimentally, however, in the case that $P_{\ell 1} \gg P_{\ell 2}$, $\tau_1 \gg \tau_2$, $\tau_1 = \tau_2$ or vice versa, only one relaxation time should be observed. If only one relaxation time is observed, one must be careful in trying to relate the observed relaxation time to the rate constants involved in the above reactions. First of all, the concentrations of the system must be checked to see if one of the two reactions is predominant. If it is, then a single step mechanism should be used to derive the expression for τ_j and the rate constants obtained are referred to that step only. Otherwise, a two-step mechanism should be used to derive the expression for the single relaxation process. Secondly, if the single relaxation process results from a single step mechanism it is necessary to yield a linear relationship between the concentration $f(c)$ and the reciprocal of relaxation times obtained at different concentrations.

III

EXPERIMENTAL

EXPERIMENTAL

1. Nature of the Temperature Jump Apparatus (41)

If a solution, initially at thermal equilibrium, is perturbed by a rapid increase in temperature, the magnitude of the concentration changes is governed by the values of ΔH° and the degree of temperature variation, according to:

$$\left(\frac{\partial \ln K}{\partial T}\right)_P = \frac{\Delta H^\circ}{RT^2}. \quad (\text{III-1})$$

In this equation, K is the equilibrium constant of the chemical reaction at constant pressure, ΔH° is the standard enthalpy change of the reaction, R is the gas constant and T is the absolute temperature. Thus, a system will be perturbed by a temperature jump if any one of a sequence of coupled reactions is characterized by a non-zero enthalpy change.

The temperature pulse is applied to a low resistance electrolyte solution by the discharge of a high voltage condenser through the solution in a suitable electrode cell. The value of the condenser, the cell resistance, the voltage at discharge, and the volume of the cell are chosen to provide a rapid change in the temperature of the contents of the cell between the electrodes. The rise time for the rapid temperature change is dictated by the properties of the electronics and the solution itself. If $\frac{RC}{2} \gg \frac{2L}{R}$, the current delivered during discharge has the overdamped form

$$i = \left(\frac{V_0}{R}\right)e^{-t/RC}. \quad (\text{III-2})$$

Here R is the resistance of the solution between the electrodes of the cell, C is the discharge capacitance in Farads, L is the inductance of the high voltage condenser, and V_0 is the initial value of the voltage across the condenser or the electrodes of the cell.

The temperature change with respect to time is related to the heat produced as follows

$$\frac{dT}{dt} = \frac{i^2 R}{4.18 C_p \rho V} \quad (\text{III-3})$$

where C_p and ρ are the specific heat capacity and density of the solution, and V is the volume of the solution between electrodes that is heated, $i^2 R$ is the heat produced when the current passes through the solution with a resistance R , and 4.18 is the factor converting joules into calories.

Substituting Equation (II-2) into Equation (II-3) and integrating from $t = 0$ to $t = t$, we have

$$\begin{aligned} \delta T(t) &= \frac{C V_0^2}{8.36 C_p \rho V} [1 - e^{-2t/RC}] \\ &= \delta T_\infty [1 - e^{-2t/RC}] \end{aligned}$$

where δT_∞ is the final temperature rise. Thus the shortest resolution time of the apparatus is a few times $\frac{RC}{2}$. The resistance of the cell can be varied by use of different concentrations of inert electrolytes. The characteristics of a temperature jump cell are shown in Table III.

TABLE III

CHARACTERISTICS OF A STANDARD TEMPERATURE JUMP CELL

light pass length	$R^{(1)}$	C	V_0	V	$\frac{RC}{2}$	δT_∞
1 cm	140 ohms	0.1 μ f	25 Kv	\sim 1c.c.	7 μ sec.	8°C

(1) Resistances when 0.1 M KNO_3 is in the cell at room temperature.

The detection of the concentration changes can be accomplished by use of absorption spectrophotometry as illustrated in Chapter II.

2. Apparatus

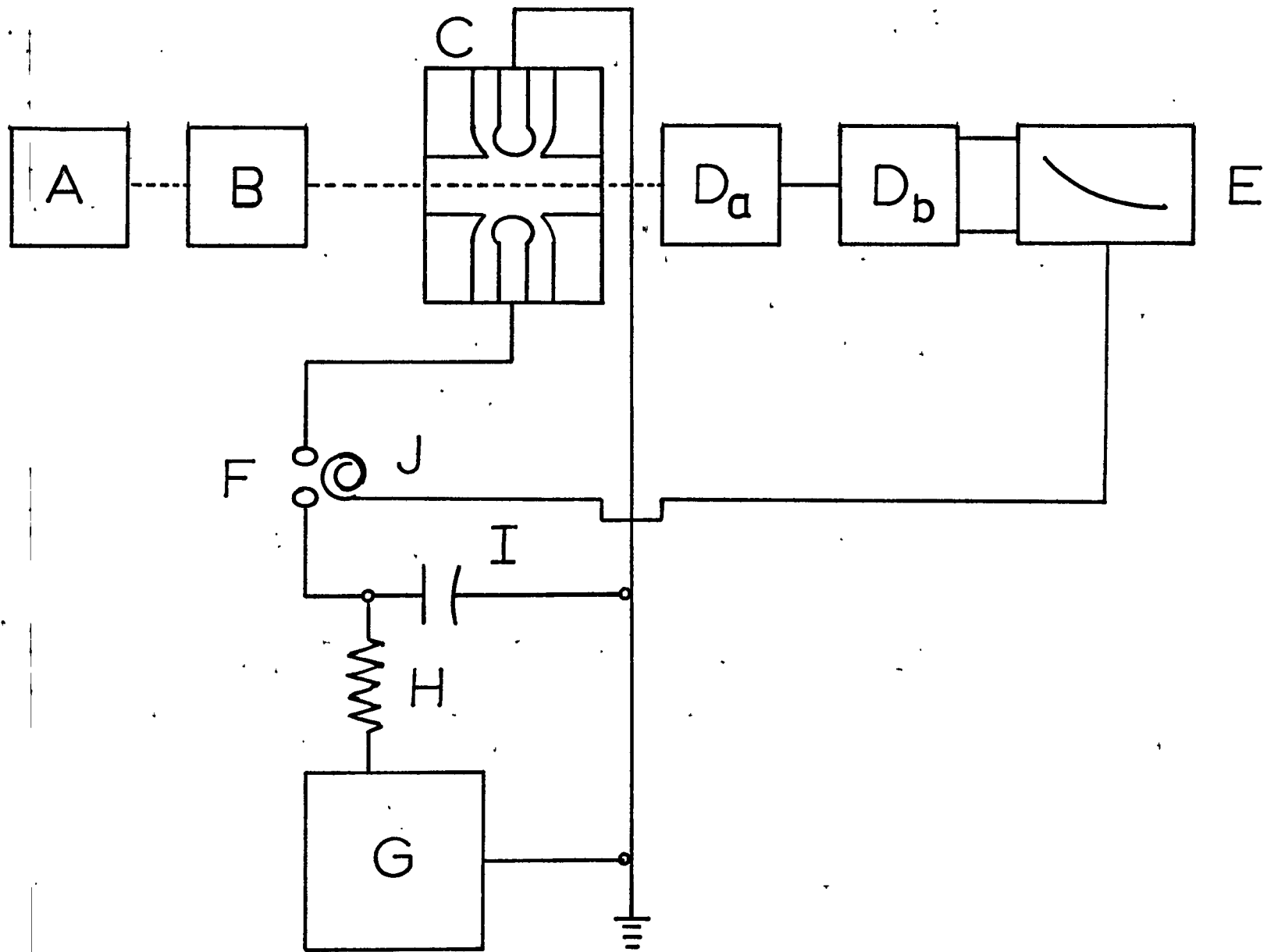
The apparatus constructed in this laboratory is similar to that described by Hammes and French (41). The apparatus consisted of three principal parts. The first part is used to initiate the temperature jump; the second part is to detect the change in reaction with the aid of a light source, a photomultiplier and a detection circuit; and the third part is to record the change between the two different equilibrium conditions by using a Polaroid camera mounted on the oscilloscope.

A simplified diagram of the temperature jump apparatus, which uses joule heating, is shown in Figure 3. The entire spark gap assembly (F), with condenser (I) and charging resistor (H) is insulated by enclosure in a polyethylene box. The polyethylene box is surrounded by two electrostatic boxes; an aluminum outer box which is grounded and a copper inner box which is connected directly to the low voltage side of the condenser and also to the ground electrode of the cell by means of the shield of a high voltage cable. The high voltage cable is used to connect the high voltage cell electrode and the condenser to the two spark electrodes, respectively. An antenna and jack (J) are mounted near the window of the polyethylene box through which the spark gap may be viewed. As soon as the condenser is discharged, the oscilloscope is triggered by the antenna which is exposed to the changing electromagnetic fields produced by the spark.

FIGURE 3

SCHEMATIC DIAGRAM OF A TEMPERATURE JUMP APPARATUS

- A = Light source
- B = Monochromator
- C = Sample cell
- D_a = Photomultiplier
- D_b = Detection Circuit
- E = Oscilloscope
- F = Spark gap
- G = High voltage power supply
- H = Charging resistor
- I = Condenser
- J = Trigger Antenna



The sample cell (C) consists of two electrodes about 0.47 inches apart and requires about 20 ml of solution. However, the volume that is heated by the electrical discharge is only 1 ml. The solution is thermostated by a constant temperature water-ethylene glycol mixture circulating directly through the ground electrode of the cell. The signal from the cell (change in absorbance) is amplified by the detection circuit.

Special attention must be paid to a suitable arrangement of the various boxes in order to prevent electromagnetic wave propagation which will interfere with the signal observed. The aluminum box housing the sample cell is placed in a coaxial arrangement directly on the top of the aluminum box housing the spark discharge circuit. The high voltage power supply lead is attached through a 2.5 cm long aluminum tube to the aluminum box enclosing the spark apparatus. This approach avoids leakage of the pulse energy outside the box via the cables. The pulsed electromagnetic fields incident on the photomultiplier through the window in the box housing the cell are attenuated by inserting a 5 cm long aluminum box with a diameter of 1.27 cm between the windows of the photomultiplier and the sample cell.

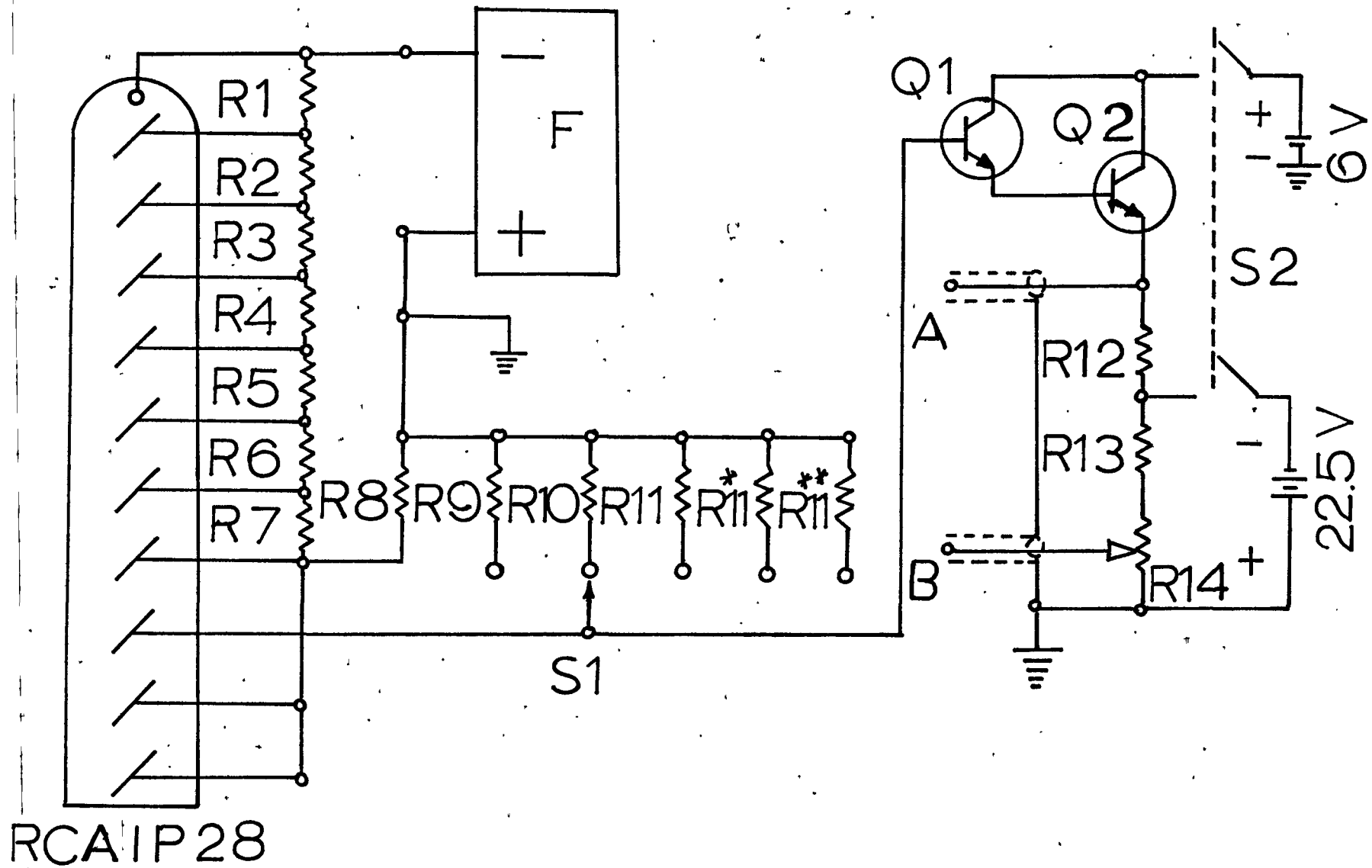
A Hitachi UV spectrophotometer is used as the light source and monochromator, and changes in light intensity can be conveniently followed with an IP-28 photomultiplier and a detection circuit (Figure 4). This circuit is adequate for measurement of relaxation times of a few microseconds when the minimum load resistor (R_9 in Figure 4) is used.

FIGURE 4

SCHEMATIC DIAGRAM OF A PHOTOMULTIPLIER
AND A DETECTION CIRCUIT

Q1, Q2, 2N336. R1, 150K Ω . R2-R9, R13, 100 K Ω .
R10, 300 K Ω . R11, 1M Ω . R*11, 50K Ω . R**11,
10 K Ω . R12, 5K Ω . All resistors are 1/2 W and
 $\pm 5\%$.

R14, 100 K Ω potentiometer, 2W, linear taper. S1,
1-pole, 3-position Ceramic rotary switch; S2,
DPST, toggle switch. F, photomultiplier power
supplier.



The cathode of the photomultiplier is connected to a well-regulated power supply (F in Figure 4). The maximum anode to cathode voltage of the photomultiplier is 1000 volts. The signal (A in Figure 4) and the reference (B in Figure 4) are connected to the input of a Tektronic Type 547 oscilloscope. Transistors Q_1 and Q_2 are powered by a 6 v DC battery and the initial photomultiplier signal is balanced by a potentiometer (R_{14} in Figure 4) which is connected to a 22.5 v DC battery. If the initial vertical position is properly balanced, a signal trace will appear on the screen of the oscilloscope at the instant of triggering.

The signal to noise ratio (S/N) of the detection circuit is given approximately by the equation,

$$\frac{S}{N} = 1.4 \times 10^9 \left(\frac{\delta I}{I} \right) \left(\frac{I_0 A_g S_\lambda}{\Delta f} \right)^{1/2} e^{-1} \frac{1}{2^{\epsilon_i} C_i} \quad (\text{III-5})$$

where $\frac{\delta I}{I}$ is the relative change in light intensity, $I_0 A_g$ is the available light intensity, S_λ is the sensitivity of the photocathode at a particular wavelength, Δf is the band width, and the other symbols have been previously defined.

In order to increase the signal to noise ratio, the light intensity at the photomultiplier cathode should be as high as possible within the region where the response of the photomultiplier to changes in light intensity is linear. Also the band width (range of frequencies) of the detection circuit should be as narrow as possible. The band width can be narrowed by increasing the load resistance of the detection

circuit ($R_g - R_{11}^{**}$, in Figure 4). Another way to increase this ratio is to remove the high frequency noise by passage of the signal (A in Figure 4) through a simple RC filter before going to the oscilloscope. In general, the increase in the ratio is accompanied by an increase in the resolution time of the apparatus.

3. Equilibrium Constant Measurements

a) Principle

The Klotz and Ming method for the determination of formation constant by spectrophotometry was employed here (42).

If the concentration of metal (\bar{C}_M) is high compared to that of the ligand (\bar{C}_L), the first stability constant, K_1 , for the formation of the 1:1 metal chelate ML, may be expressed as

$$M + L \rightleftharpoons ML$$

$$K_1 = \frac{\bar{C}_{ML}}{\bar{C}_M \cdot \bar{C}_L} = \frac{\alpha C_L}{(C_M - \alpha C_L)(1-\alpha)C_L} = \frac{\alpha}{(C_M - \alpha C_L)(1-\alpha)} \quad (\text{III-6})$$

where C_M and C_L represent the initial molar concentrations of the metal ion and the ligand respectively, and α , the fraction of the ligand bound to the metal ion. The value of α is determined spectrophotometrically.

According to Beer's law, in any given mixture the observed optical density, $\log \left(\frac{I_0}{I} \right)$ total, is the sum of the contributions of each species, represented by the appropriate subscript in the equation.

$$\log \left(\frac{I_0}{I} \right)_{\text{total}} = \log \left(\frac{I_0}{I} \right)_M + \log \left(\frac{I_0}{I} \right)_{ML} + \log \left(\frac{I_0}{I} \right)_L \quad (\text{III-7})$$

Here I_0 is the light intensity emerging from the solvent, and I is the light intensity emerging from the solvent containing the species as indicated by the subscripts only. If d is the thickness of the cell in centimeters and ϵ_{ML} is the extinction coefficient of ML, and ϵ_L is the corresponding value for L at the same wavelength, then

$$\log \left(\frac{I_0}{I} \right)_{\text{total}} - \log \left(\frac{I_0}{I} \right)_M = \epsilon_L \cdot \bar{C}_L \cdot d + \epsilon_{ML} \cdot \bar{C}_{ML} \cdot d \quad (\text{III-8})$$

since $\bar{C}_L = (1 - \alpha) C_L$ and $\bar{C}_{ML} = \alpha C_L$, then Equation (III-8) becomes

$$\frac{\log \left(\frac{I_0}{I} \right)_{\text{total}} - \log \left(\frac{I_0}{I} \right)_M - \epsilon_L C_L d}{(\epsilon_{ML} - \epsilon_L) C_L \cdot d} = \alpha \quad (\text{III-9})$$

In practice, $\log \left(\frac{I_0}{I} \right)_M$ is negligible compared to $\log \left(\frac{I_0}{I} \right)_{\text{total}}$ measured in this experiment. The value for ϵ_L may be obtained directly from the optical density of a solution containing ligand alone at a known concentration and a selected wavelength. Values for ϵ_{ML} can be obtained by an extrapolation method. For a set of solutions containing the same total concentration of ligand, the optical density increases with increase in metal ion concentration as a consequence of the increased amounts of metal chelate, when optical density is measured at the wavelength of the absorption maximum for ML. The concentration of ligand will approach zero when the concentration of metal ion is

further increased. Equation (III-8) can be simplified as

$$\log \left(\frac{I_0}{I} \right)_{\text{total}} - \log \left(\frac{I_0}{I} \right)_M \approx \epsilon_{ML} \cdot \bar{c}_{ML} \cdot d \quad (\text{III-10})$$

The value of $\log \left(\frac{I_0}{I} \right)_M$ may be obtained from a separate set of absorption measurements in solution containing the free metal ion at the same total concentration as in the chelate-containing solution. This term contributes a few percentages of the over-all optical density even at the highest metal ion concentration used. Thus, the stability constants can be evaluated from Equations (III-6) and (III-9).

b) Preparation of the Solutions

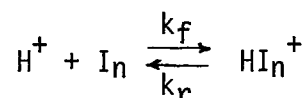
All of the inorganic chemicals used were of reagent grade quality. The stock solutions of lanthanide perchlorate and nickel(II) chloride were standardized by an ion exchange technique. A standardized NaOH solution of known volume was added in advance to make the pH values of the lanthanide stock solutions between 3 and 4. The initial nickel(II) chloride solution was of the order of 0.1 M while the lanthanide perchlorate solution was about 10^{-3} M. The desired concentrations were obtained by dilution of the stock solutions. Absolute ethanol, DMSO, and murexide were used without further purification. Sodium perchlorate was used to regulate the ionic strength of all the final solutions to 0.1 M except in H_2O and H_2O - DMSO mixture where KCl and/or NaClO_4 were used. The final solutions were freshly prepared for each determination by weighing murexide into the diluted metal ion solution. It took about 30 minutes to dissolve the

murexide powder, and the resulting solutions were stable for several hours. The pH was adjusted by dropwise addition of solutions of NaOH and/or HClO_4 . The final pH value was measured on a Beckman research model pH meter. Absorption spectra and optical density were determined at different temperatures with a Hitachi UV spectrophotometer using one centimeter path length cells.

4. Kinetic Measurements

The test solutions were freshly prepared and placed into the sample cell, the electrical connections were checked and the optical elements were adjusted. The linearity of the signal against the light intensity should be examined using a neutral density filter with known transmittance. The total signal change between light and dark which is generally 2 volts was measured by blocking the light source. This can be accomplished by varying the voltage of the power supply for the photomultiplier. The noise level of the signal was 5 mV/cm. The desired load resistor and filter capacitor were chosen such that the resolution time of the apparatus be less than one-tenth of the relaxation time being measured. The resolution time of the apparatus is measured by studying a very fast indicator protolytic reaction. Some rate constants and other properties of indicators are collected in Table IV, whereas typical resolution times of the apparatus under different conditions are shown in Figures 5 and 6. When the resolution time is of the same order of magnitude as the relaxation time being measured, it is necessary to correct the observed value by use of the following equation.

TABLE IV
 RATE CONSTANTS AND λ_{\max} AND ϵ_{\max}
 OF SOME INDICATORS



Indicator	$k_f (M^{-1} \text{sec}^{-1})$	$\lambda_{\max} (\text{nm})$	ϵ_{\max}
Phenolphthalein	---	550-555	26500
Phenol red	3×10^{11}	560	63000
Bromothymol blue	---	617-620	36300
Introphenol	3.6×10^{10}	430	8200
Bromocresol green	---	610-614 (pH>7)	43000
Chlorophenol red	2.3×10^{11}	573	44000
Methyl red	3.5×10^{10}	440 (pH>6)	15000
Barbital	4.2×10^{10}	---	--
Cresol red	4×10^9	---	--
Imidazole	1.5×10^{10}	---	--
Bromochlorophenol blue	---	590	--

FIGURE 5

TEMPERATURE JUMP OSCILLOGRAM FOR AN AQUEOUS $10^{-5}M$
PHENOLPHTHALEIN IN 0.1 M KNO_3 SOLUTION
WITH pH 9.2 AT ROOM TEMPERATURE

Sweep rate = 20μ sec/cm

Sensitivity = 20 mv/cm

Load resistance = 100 $K\Omega$

No filter capacitor used

FIGURE 6

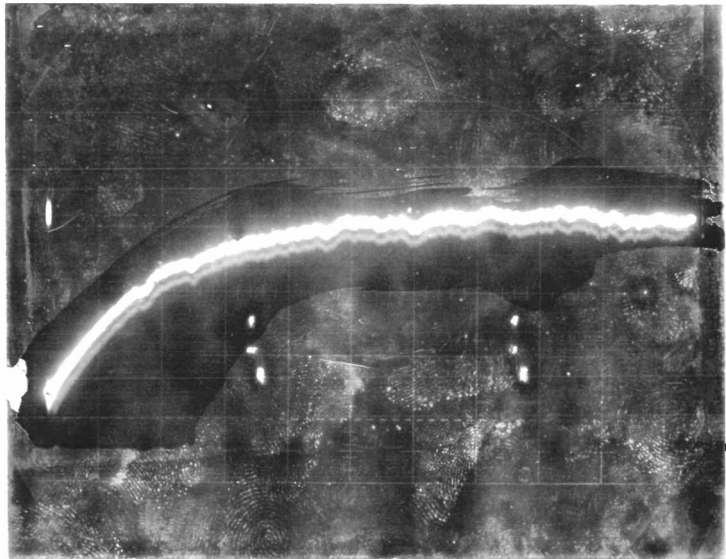
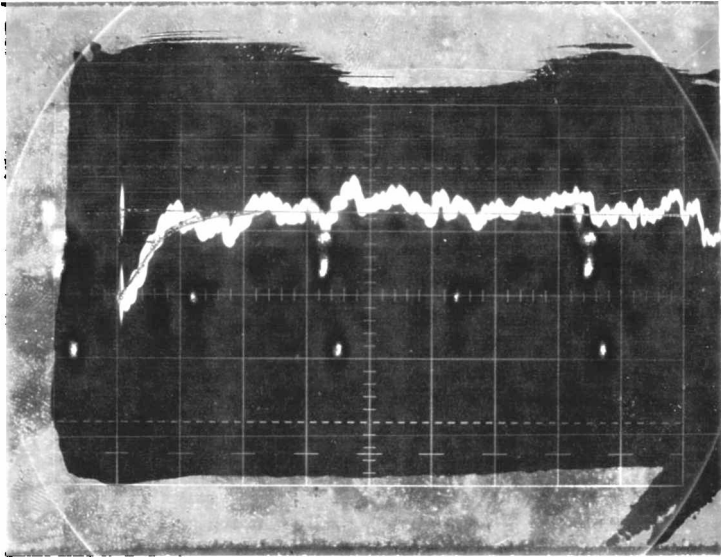
TEMPERATURE JUMP OSCILLOGRAM FOR AN AQUEOUS $6 \times 10^{-5}M$
PHENOLPHTHALEIN IN 0.1 M KNO_3 SOLUTION
WITH pH 9.2 AT ROOM TEMPERATURE

Sweep rate = 20μ sec/cm

Sensitivity = 20 mv/cm

Load resistance = 300 $K\Omega$

Capacitor = 2μ farads



$$\frac{1}{e} = \left(\frac{1}{\tau_i - \tau_s} \right) [\tau_i e^{-t/\tau_i} - \tau_s e^{-t/\tau_s}] \quad (\text{III-11})$$

where t refers to measured relaxation time, τ_s resolution time of the apparatus, and τ_i relaxation time of the chemical reaction studied. The chemical relaxation time was determined for different concentrations at each temperature. Typical oscillograms of relaxation process are given in Figures 7-17. Blank experiments with solutions containing only the metal ion or the ligand did not show any relaxation effect under the present experimental conditions. The concentrations of the metal ion, ligand, and complexes were calculated from the stability constants previously determined. The kinetic parameters and rate constants were evaluated according to the mechanism proposed.

FIGURE 7
EXPERIMENTAL RELAXATION
CURVE FOR NICKEL(II) MUREXIDE

Temperature = 21°C pH = 5
Ionic strength = 0.1 M, $\text{Ni}^{++} = 6 \times 10^{-4}$ M
Murexide = 10^{-4} M, Solvent composition = H_2O
Relaxation time = 500 msec (not average value)

FIGURE 8
EXPERIMENTAL RELAXATION
CURVE FOR NICKEL(II) MUREXIDE

Temperature = 31.5°C, pH = 5
Ionic strength = 0.1 M, $\text{Ni}^{++} = 6 \times 10^{-4}$ M
Murexide = 10^{-4} M, Solvent composition = H_2O
Relaxation time = 250 msec (not average value)

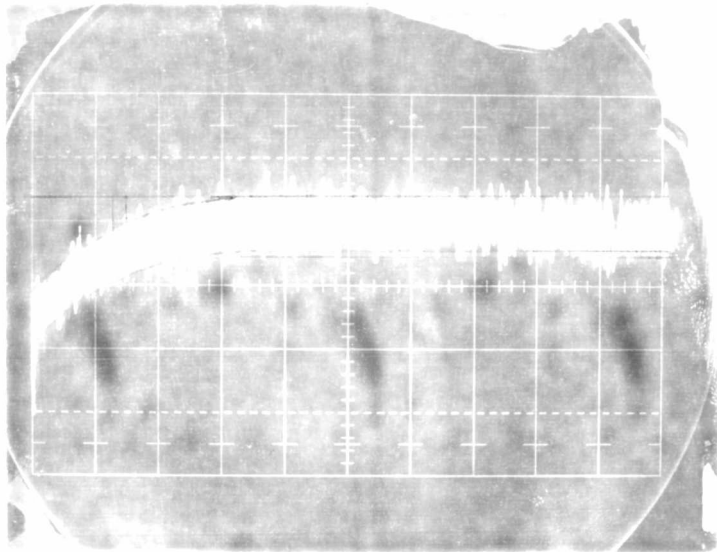
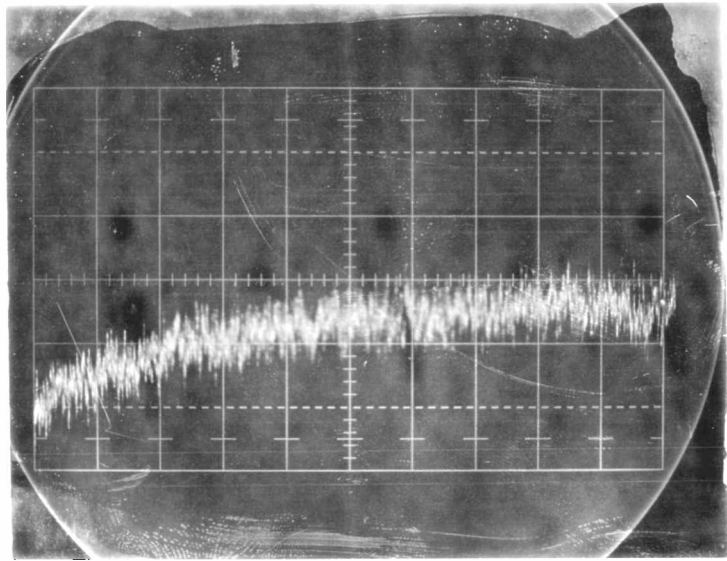


FIGURE 9
EXPERIMENTAL RELAXATION
CURVE FOR NICKEL(II) MUREXIDE

Temperature = 31.5°C, pH = 5
Ionic strength = 0.1 M, Ni⁺⁺ = 3.3×10^{-4} M
Murexide = 10^{-4} M, Solvent composition =
25% DMSO aqueous solution
Relaxation time = 360 msec (not average value)

FIGURE 10
EXPERIMENTAL RELAXATION
CURVE FOR NICKEL(II) MUREXIDE

Temperature = 31.5°C, pH = 5
Ionic strength = 0.1 M, Ni⁺⁺ = 1×10^{-3} M
Murexide = 10^{-4} M, Solvent composition =
25% DMSO aqueous solution
Relaxation time = 176 msec (not average value)

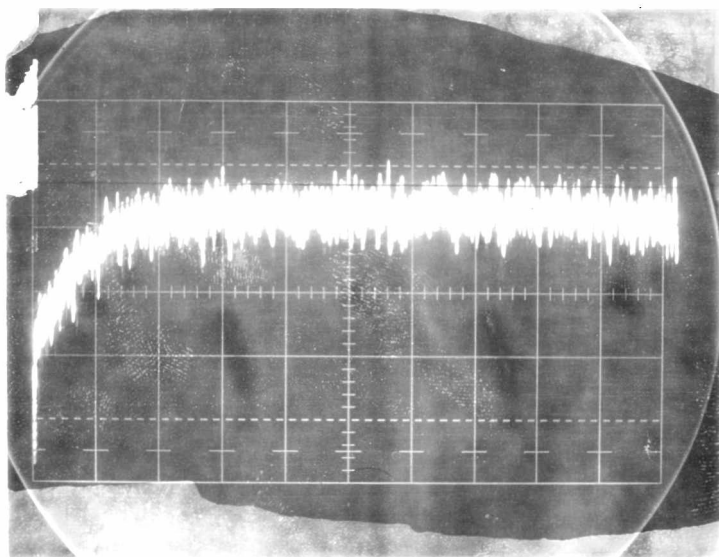
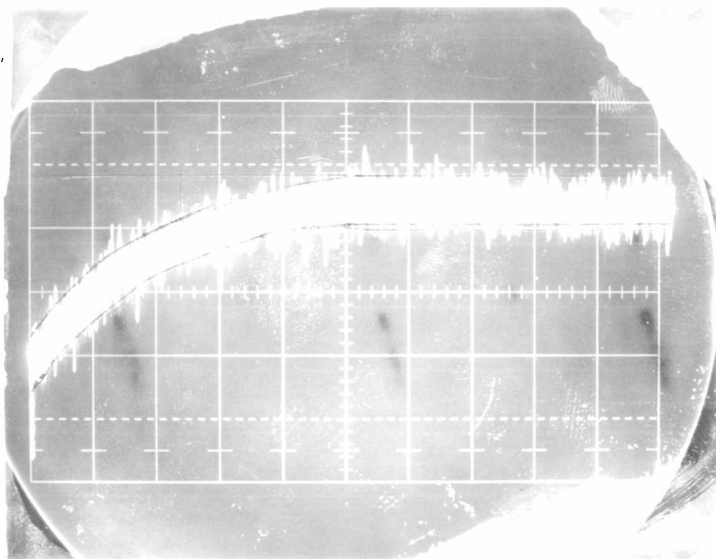


FIGURE 11

EXPERIMENTAL RELAXATION
CURVE FOR NICKEL(II) MUREXIDE

Temperature = 31.5°C, pH = 5
Ionic strength = 0.1 M, Ni⁺⁺ = 6.5×10^{-4} M
Murexide = 6×10^{-5} M, Solvent composition =
50% DMSO aqueous solution
Relaxation time = 248 msec (not average value)

FIGURE 12

EXPERIMENTAL RELAXATION
CURVE FOR NICKEL(II) MUREXIDE

Temperature = 40°C, pH = 5
Ionic strength = 0.1 M, Ni⁺⁺ = 5×10^{-4} M
Murexide = 5×10^{-5} M, Solvent composition =
50% DMSO aqueous solution
Relaxation time = 140 msec (not average value)

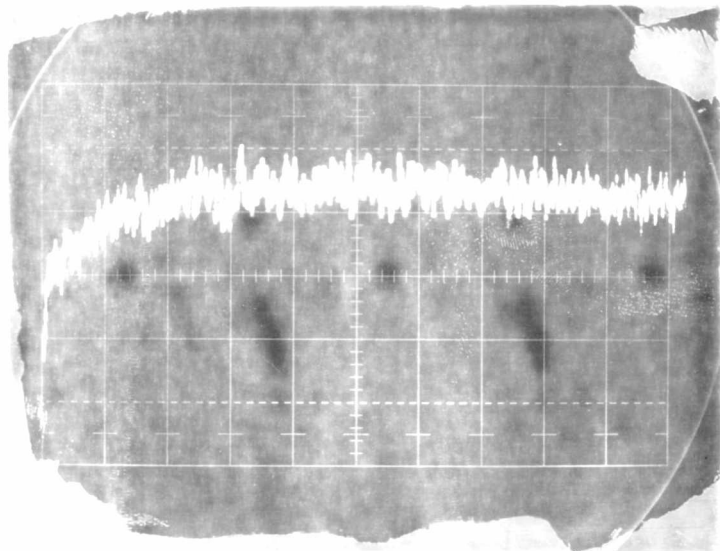
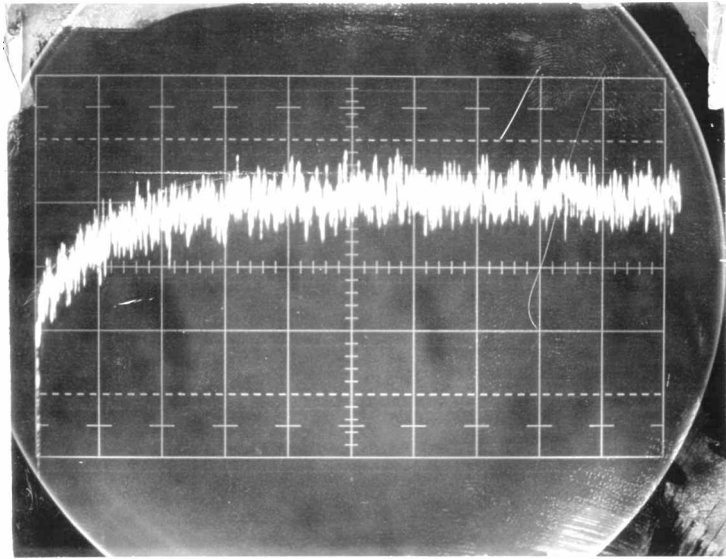


FIGURE 13

EXPERIMENTAL RELAXATION
CURVE FOR NICKEL(II) MUREXIDE

Temperature = 25°C, pH = 5
Ionic strength = 0.1 M, $\text{Ni}^{++} = 4 \times 10^{-4}$
Murexide = 5×10^{-5} , Solvent composition =
50% ethanol aqueous solution
Relaxation time = 267 msec

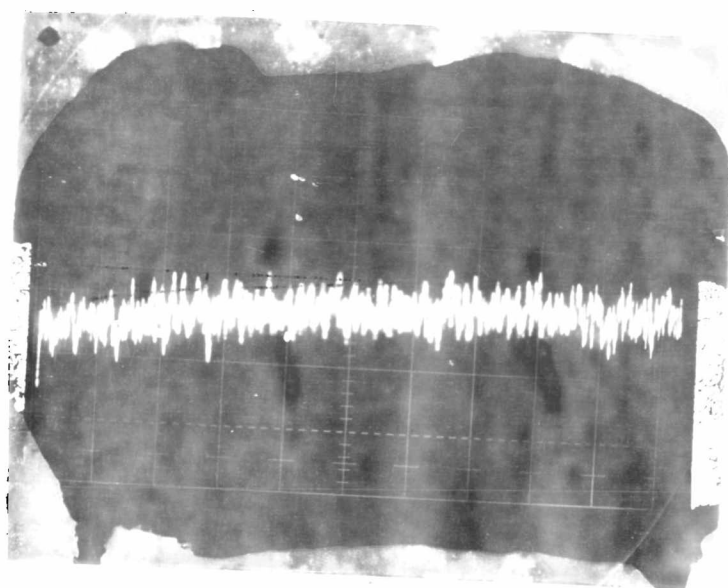


FIGURE 14

EXPERIMENTAL RELAXATION
CURVE FOR TERBIUM(III) MUREXIDE

Temperature = 12°C, pH = 5
Ionic strength = 0.1 M, $Tb^{+3} = 4 \times 10^{-5}$ M
Murexide = 2×10^{-5} M
Solvent composition = 50% ethanol aqueous solution
Corrected relaxation time = 550 μ sec (average value \pm about 30%)

FIGURE 15

EXPERIMENTAL RELAXATION
CURVE FOR GADOLINIUM(III) MUREXIDE

Temperature = 12°C, pH = 5
Ionic strength = 0.1 M, $Gd^{+3} = 4 \times 10^{-5}$ M
Murexide = 2×10^{-5} M
Solvent composition = 50% ethanol aqueous solution
Corrected relaxation time = 410 μ sec (average value \pm about 30%)

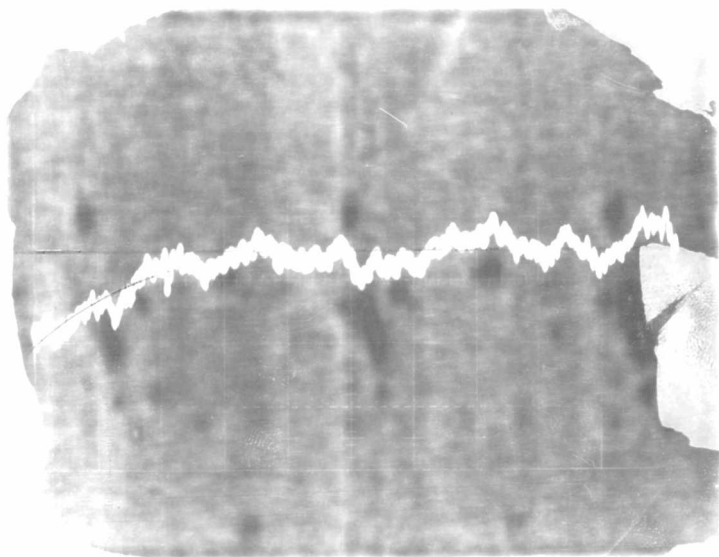
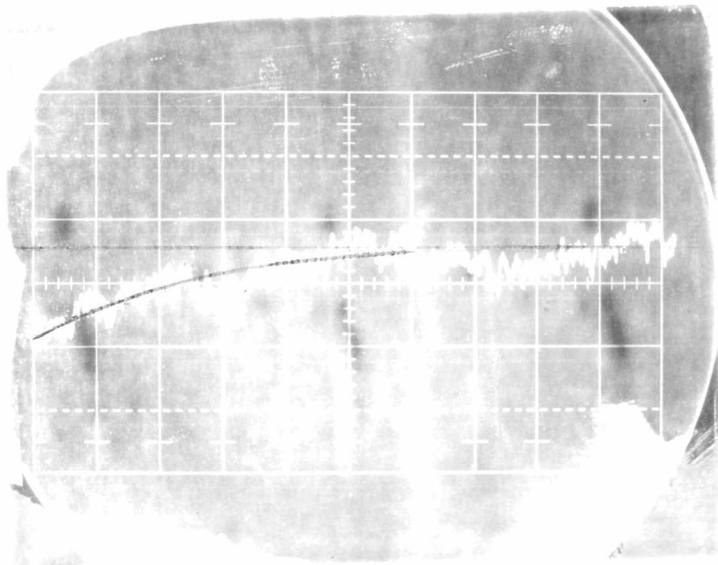


FIGURE 16

EXPERIMENTAL RELAXATION

CURVE FOR HOLMIUM(III) MUREXIDE

Temperature = 12°C, pH = 5

Ionic strength = 0.1 M, $\text{Ho}^{+3} = 2.5 \times 10^{-5}$ M

Murexide = 1×10^{-5} M

Solvent composition = 50% ethanol aqueous solution

Corrected relaxation time = 800 μsec (average value \pm about 30%)

FIGURE 17

EXPERIMENTAL RELAXATION

CURVE FOR DYSPROSIUM(III) MUREXIDE

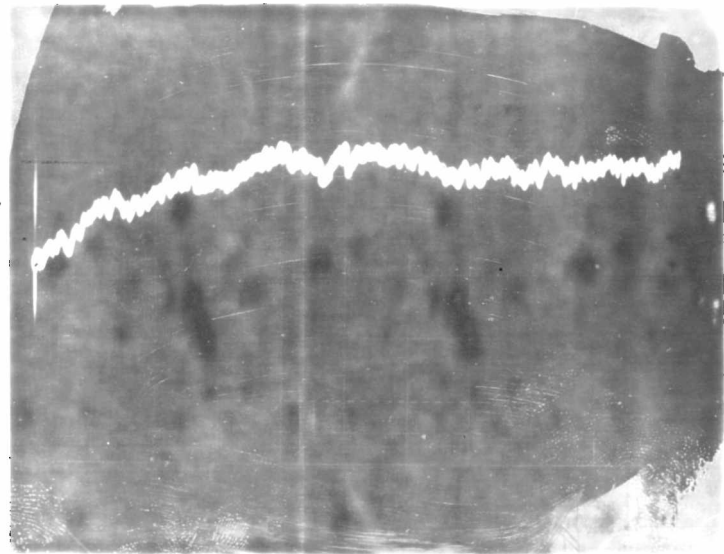
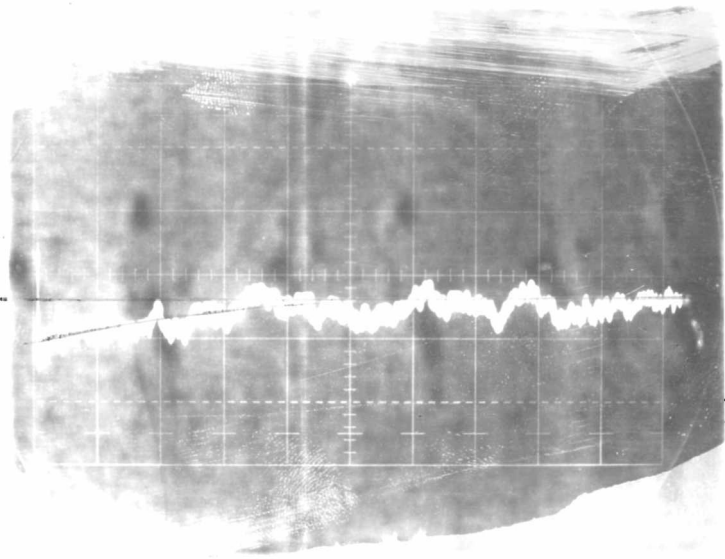
Temperature = 12°C, pH = 5

Ionic strength = 0.1 M, $\text{Dy}^{+3} = 4 \times 10^{-5}$ M

Murexide = 2.4×10^{-5} M

Solvent composition = 50% ethanol aqueous solution

Corrected relaxation time = 560 μsec (average value \pm about 30%)



IV

RESULTS AND DISCUSSION

RESULTS AND DISCUSSION

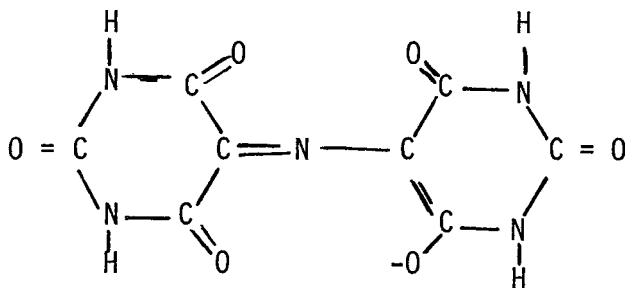
1. Thermodynamic Section

The stability constants have been determined for nickel(II), holmium(III), dysprosium(III), gadolinium(III), samarium(III) and europium(III) with murexide in water and mixed solvents at several temperatures. A similar determination has been made by Gier (24) at a single temperature and in aqueous solution under different conditions.

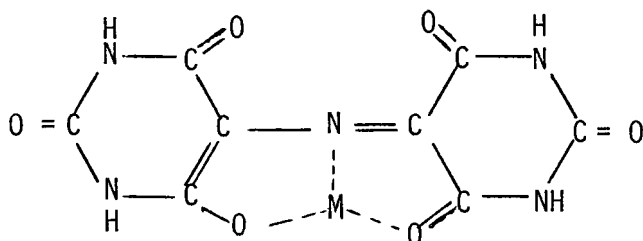
It is well known that murexide may be used as an end-point indicator for metal-EDTA titrations. Schwarzenbach (43,44,45) has described three forms of this dye. The equilibrium for these species is



A solution of murexide is red-violet below pH 9, violet from pH 9 to 11, and blue above pH 11. The monovalent anion will be protonated at about pH 2. The structure of the perpureate ion (H_2L^{-1}) and its chelates are given as follows (45):



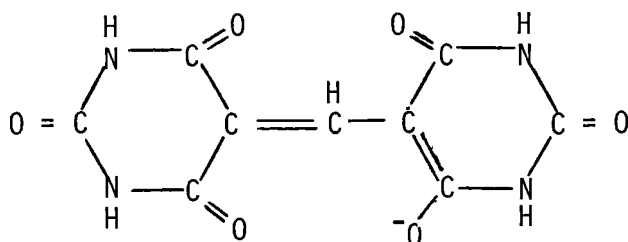
I. Perpureate Ion



II. Perpurreate Chelate

The peaks of the maximum absorption bands are raised and shifted toward the ultraviolet region when the perpurreate ion is chelated.

It has been suggested (46) that chelate formation involves binding of the electron pair on the nitrogen atom between the two rings, since the chelates all show absorption bands intermediate between that of perpurreate ion and the corresponding methine (Formula III). The difference in color between the perpurreate ion and the methine is believed to be caused by the absence of the free electron pair of the nitrogen atom in the methine.

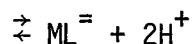


III. Methine

The pK values for the acid dissociation constants of the murexide are decreased by the chelation of the acid with the metal ion (46). The strong donation of electrons to the metal ion renders the donor

groups considerably more positive, and this is transmitted to the imide nitrogen atoms through inductive and resonance effects. Thus, the pH ranges must be well established before the stability constants are determined.

Only the stability constant between the metal ion and the perpureate ion of murexide is of interest. The other two equilibria shown in Equations (IV -2) and (IV -3) can be avoided by adjusting the pH values of the solutions such that the spectra of the solutions containing the metal and perpureate ion will remain the same within a certain range of pH values , as given by:



The charges on the complexes and ligand are omitted for convenience. The spectra of nickel(II) murexide in H₂O, 25% aqueous DMSO, 50% aqueous DMSO and 50% aqueous ethanol are shown in Figures 18 - 20, respectively, whereas the transmittance for the terbium murexide system is shown in Table V. All spectra are measured for the same metal and ligand concentrations under different pH values. All the metal murexides are complexes formed by perpureate ion and the respective metal ions.

From these figures and the information in Table V, λ_{max} for the metal chelates and working pH values were obtained. The acid dissociation constants for ^{the}perpureate ion do not vary significantly in the various

FIGURE 18

ABSORPTION SPECTRA OF NICKEL(II) MUREXIDE
AT VARIOUS pH VALUES IN AQUEOUS SOLUTION

$$\text{Ni}^{++} = 5 \times 10^{-4} \text{ M}, \quad \text{Murexide} = 10^{-4} \text{ M}$$

$$a = \text{pH } 7.40, \quad b = \text{pH } 5.35, \quad c = \text{pH } 4.75$$

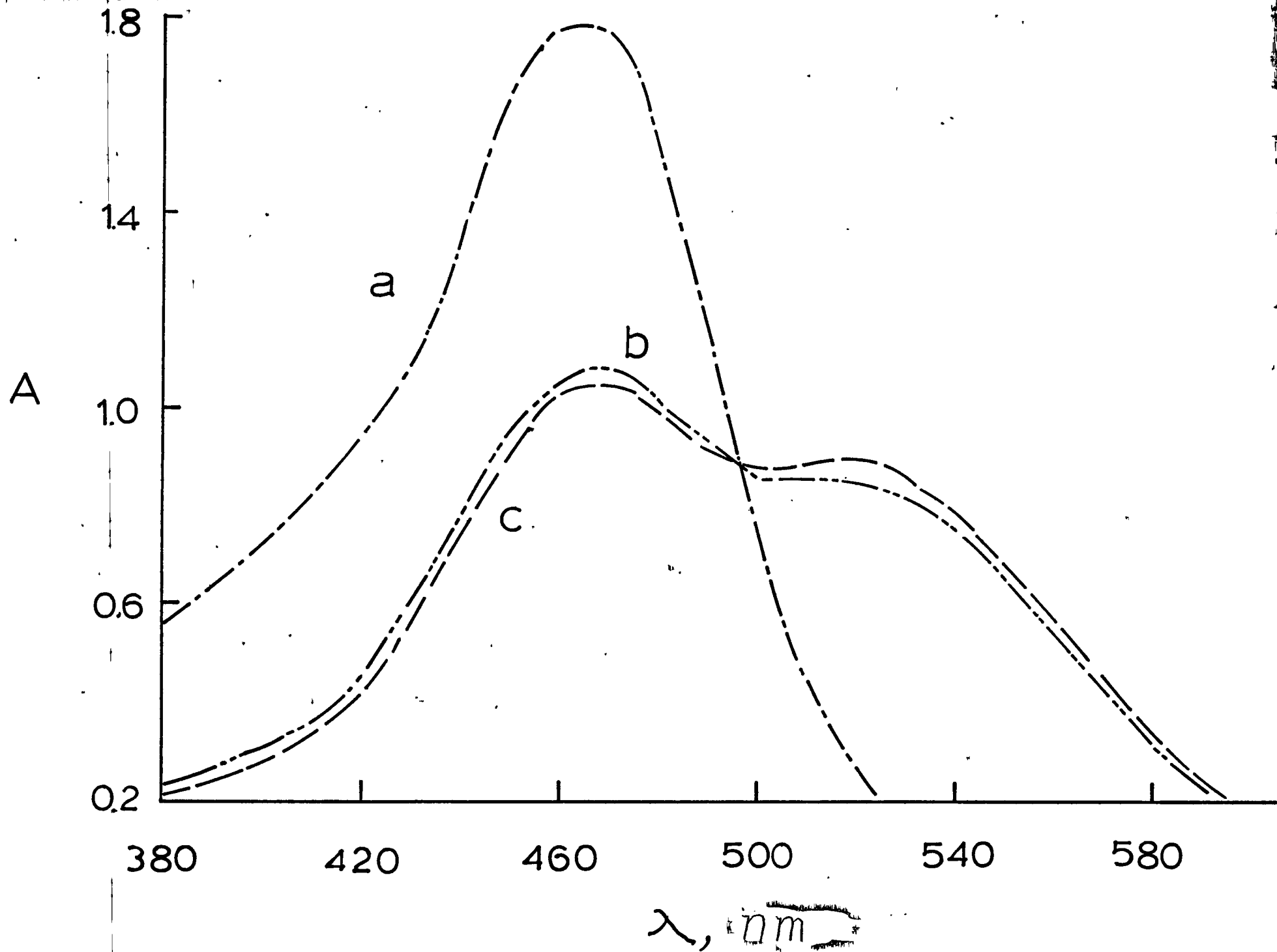


FIGURE 19

ABSORPTION SPECTRA OF NICKEL(II) MUREXIDE
AT VARIOUS pH VALUES IN 25% DMSO AQUEOUS SOLUTION

$$\text{Ni}^{++} = 5 \times 10^{-4} \text{ M}, \quad \text{Murexide} = 10^{-4} \text{ M}$$

$$a = \text{pH } 7.40, \quad b = \text{pH } 4.95 - 5.25$$

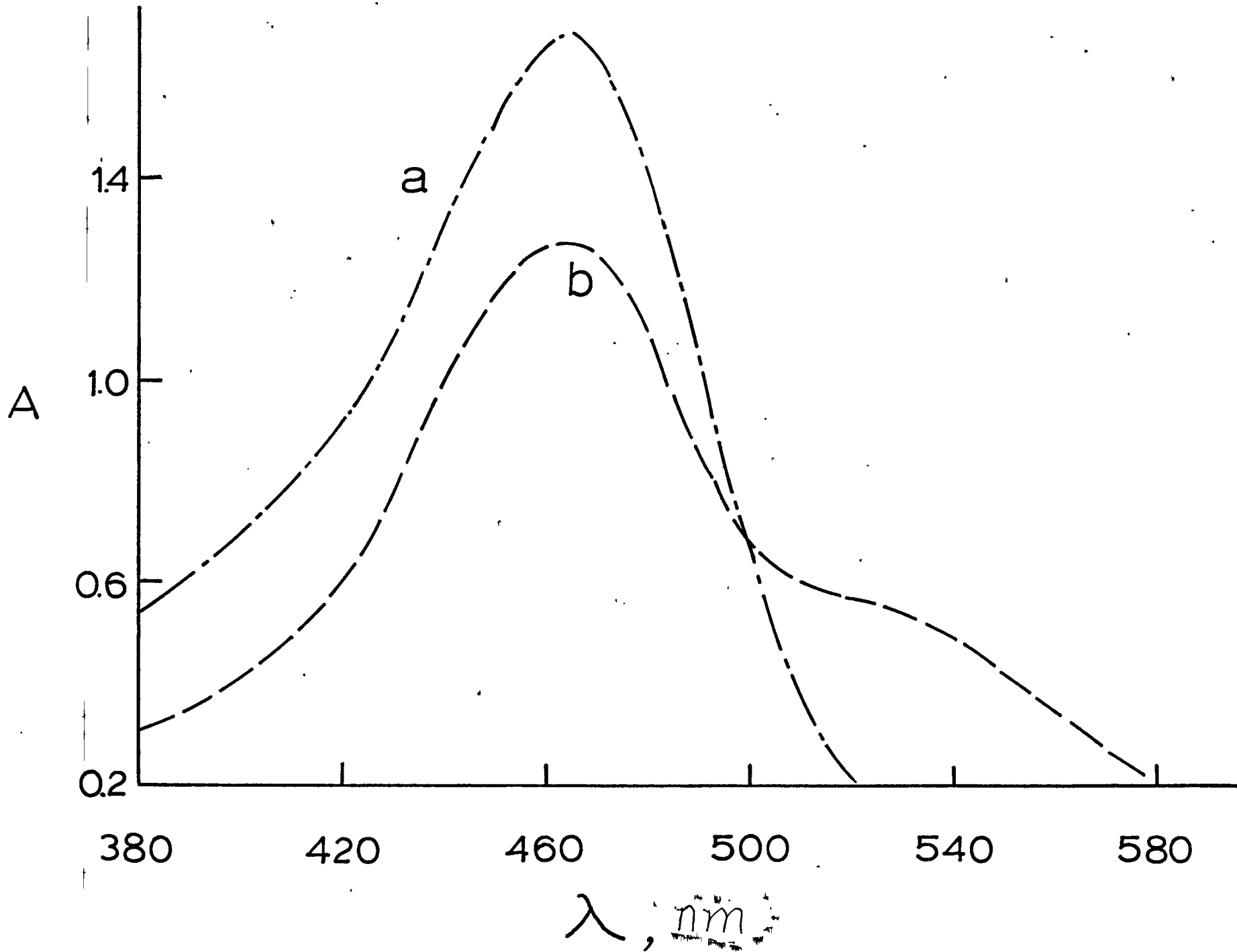


FIGURE 20

ABSORPTION SPECTRA OF NICKEL(II) MUREXIDE
AT VARIOUS pH's IN 50% DMSO AND 50%
ETHANOL AQUEOUS SOLUTIONS

- a. $\text{Ni}^{++} = 3 \times 10^{-4} \text{ M}$, Murexide = 10^{-4} , pH = 7.60
Solvent composition = 50% DMSO - H_2O
- b. $\text{Ni}^{++} = 3 \times 10^{-4} \text{ M}$, Murexide = 10^{-4} M , pH = 4.95 - 5.35
Solvent composition = 50% DMSO - H_2O
- c. $\text{Ni}^{++} = 4 \times 10^{-4} \text{ M}$, Murexide = $5 \times 10^{-5} \text{ M}$, pH = 4.70 - 5.30
Solvent composition = 50% ethanol - H_2O

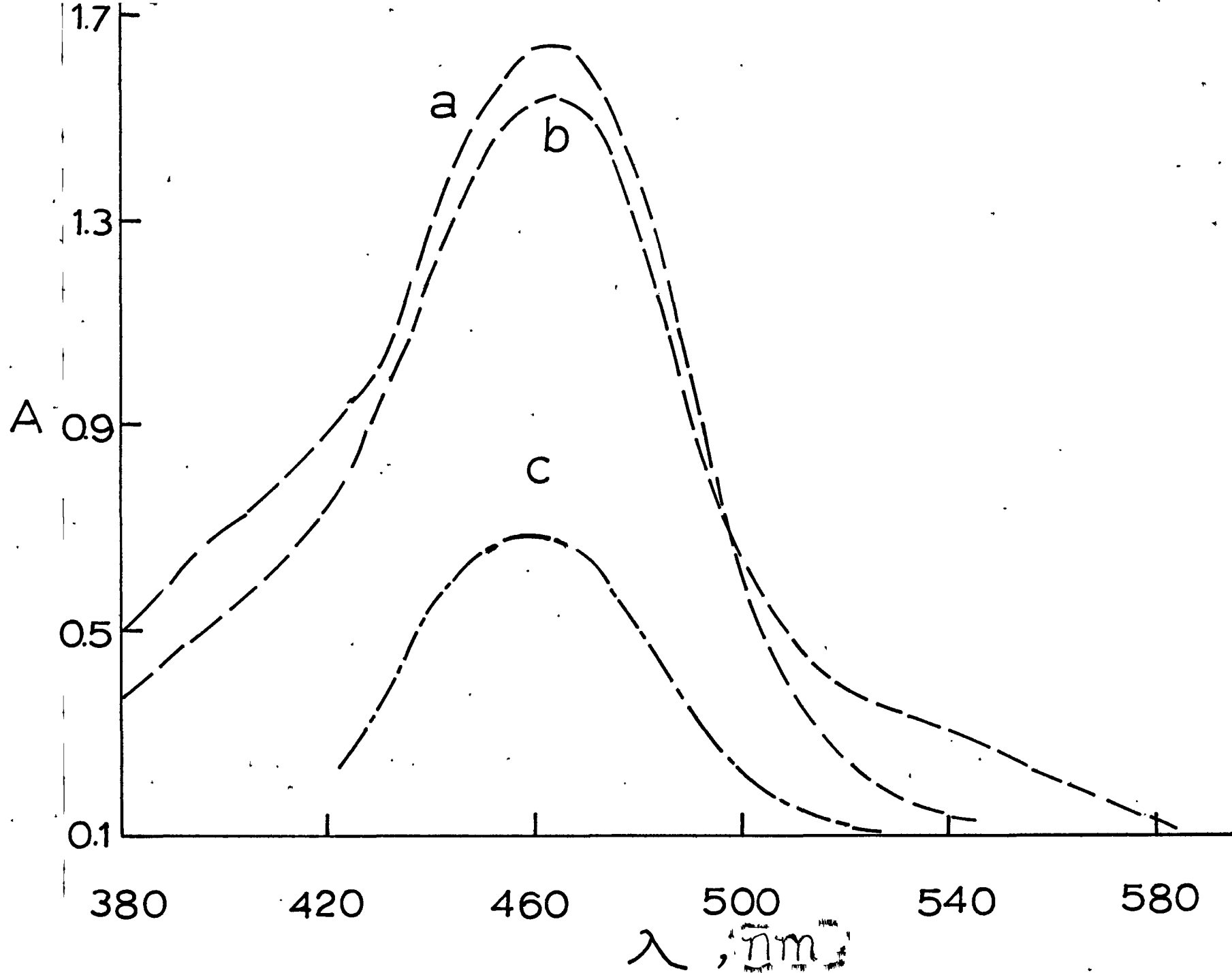


TABLE V
TRANSMITTANCE OF TERBIUM(III) MUREXIDE
IN 50% ETHANOL AQUEOUS SOLUTION AS A
FUNCTION OF pH AND WAVELENGTH

$$[\text{Tb}^{+3}] = 3 \times 10^{-5} \text{ M}$$
$$[\text{Murexide}] = 0.5 \times 10^{-5} \text{ M}$$

Wavelength, nm	pH = 4.7	pH = 5	pH = 5.3
450	88.8%	89.8	89.2
470	84%	85.2	84.5
490	85.2%	86.4	86
510	93%	93.5	93.2
530	89.6%	90.6	90.2

solvent systems used. The molecular extinction coefficients, ϵ_L and ϵ_{ML} , used in the computations of K_1 are assembled in Table VI. They are an average of several measurements. The K_1 values calculated as described above and the optical measurements at constant temperature are given in Tables VII - XVI.

The stability constants for the mono-complex formation (Equation III-4) studied by the conductance method have been found to agree with Equation (III-5)(47), or that is,



$$K_1 = \frac{[\bar{C}_{ML}]_o + [\bar{C}_{ML}]}{(\bar{C}_M)(\bar{C}_L)} = K_o + \frac{\bar{C}_{ML}}{(\bar{C}_M)(\bar{C}_L)} \quad (IV-5)$$

where \bar{C}_{ML_o} and \bar{C}_{ML} are equilibrium concentrations for the respective outer sphere and inner sphere complexes. The corresponding free metal ion and free ligand concentrations are \bar{C}_M and \bar{C}_L . In the spectrophotometric determination, the concentrations of the outer sphere ion pair apparently have not been included. However, the elimination of the outer sphere ion pair is justified by a theoretical calculation of K_o values. It has been found that K_o is several orders of magnitude less than the K_1 obtained experimentally.

The stability constant measurements were made for nickel murexide in water and in 50% aqueous DMSO at three temperatures. The enthalpy and entropy changes for the complex formation reaction were calculated using the following equations:

TABLE VI
 MOLECULAR EXTINCTION COEFFICIENTS OF
 CHELATES AND PERPUREATE ION

Complexing metal	Solvent system	ϵ	λ_{\max} (nm)
None (free ligand)	H ₂ O	1.50x10 ⁴	520
Ni ⁺² (pH = 5)	H ₂ O	2.07x10 ⁴	460
Ni ⁺² (pH = 5)	25% DMSO - H ₂ O	2.19x10 ⁴	460
Ni ⁺² (pH = 5.2)	50% DMSO - H ₂ O	2.03x10 ⁴	460
Ni ⁺² (pH = 5)	50% ethanol - H ₂ O	1.65x10 ⁴	460
Ho ⁺³ (pH = 5)	50% ethanol - H ₂ O	2.12x10 ⁴	470
Dy ⁺³ (pH = 5)	50% ethanol - H ₂ O	2.12x10 ⁴	470
Tb ⁺³ (pH = 5)	50% ethanol - H ₂ O	2.08x10 ⁴	470
Gd ⁺³ (pH = 5)	50% ethanol - H ₂ O	1.97x10 ⁴	470
Sm ⁺³ (pH = 5)	50% ethanol - H ₂ O	2.00x10 ⁴	470
Eu ⁺³ (pH = 5)	50% ethanol - H ₂ O	2.00x10 ⁴	470
None (free ligand)	H ₂ O	0.40x10 ⁴ (460nm)	---
None (free ligand)	25% DMSO - H ₂ O	0.34x10 ⁴ (460nm)	---
None (free ligand)	50% DMSO - H ₂ O	0.34x10 ⁴ (460nm)	---
None (free ligand)	50% ethanol - H ₂ O	0.71x10 ⁴ (470nm)	---
None (free ligand)	50% ethanol - H ₂ O	0.48x10 ⁴ (460nm)	---

TABLE VII

STABILITY CONSTANTS FOR THE 1:1 NICKEL(II) MUREXIDE
 IN AQUEOUS SOLUTION AT $\lambda = 460 \text{ nm}$, IONIC STRENGTH = 0.1 M AND pH = 5

$[\text{Ni}^{+2}](\text{M})$	$[\text{H}_2\text{L}^{-1}](\text{M})$	Temperature = 12°C		Temperature = 20°C		Temperature = 32°C	
		T	$K_1 \times 10^{-3}$	T	$K_1 \times 10^{-3}$	T	$K_1 \times 10^{-3}$
8×10^{-4}	0.5×10^{-4}	19.5	2.03	20.0	1.92	25.7	1.13
		22.6	1.48	23.2	1.41	----	----
4×10^{-4}	0.5×10^{-4}	29.6	1.71	30.8	1.56	30	1.65
		27.8	1.96	28.7	1.81	----	----
2×10^{-4}	0.5×10^{-4}	----	----	40.2	1.65	41.4	1.54
		39.5	1.58	40.2	1.65	----	----
$K_1 \times 10^{-3}$ (average)		1.75		1.65		1.44	

Standard deviation in $K_1 = 10\% - 15\%$

T = Transmittance%

TABLE VIII

STABILITY CONSTANTS FOR THE 1:1 NICKEL(II) MUREXIDE
 IN 50% DMSO AQUEOUS SOLUTION AT $\lambda = 460$ nm, IONIC STRENGTH = 0.1 M AND pH = 5.3

$[\text{Ni}^{+2}](\text{M})$	$[\text{H}_2\text{L}^-](\text{M})$	Temperature = 12°C		Temperature = 20°C		Temperature = 32°C	
		T	$K_1 \times 10^{-4}$	T	$K_1 \times 10^{-4}$	T	$K_1 \times 10^{-4}$
2×10^{-4}	1×10^{-5}	70.6	1.23	71.5	1.06	73.4	0.77
		----	----	70.3	1.29	72.4	0.90
1×10^{-4}	1×10^{-5}	74.5	1.37	75.5	1.18	78.5	0.76
		73.6	1.56	75.6	1.15	78.6	0.76
5×10^{-5}	1×10^{-5}	79.5	1.43	80.6	1.21	83.4	0.75
		78.6	1.58	80.0	1.30	83.5	0.75
$K_1 \times 10^{-4}$ (average)		1.44		1.2		0.78	

Standard deviation in $K_1 = 8\% - 10\%$

T = Transmittance %

TABLE IX

STABILITY CONSTANTS FOR THE 1:1 NICKEL(II) MUREXIDE
 IN 25% AQUEOUS DMSO SOLUTIONS AT $\lambda = 460$ nm
 TEMPERATURE = 25°C, IONIC STRENGTH = 0.1 M AND pH = 5

$[\text{Ni}^{+2}](\text{M})$	$[\text{H}_2\text{L}^-](\text{M})$	Transmittance %	$K_1 \times 10^{-3}$
10^{-3}	10^{-4}	2.0	2.7
8×10^{-4}	10^{-4}	2.3	3.0
5×10^{-4}	10^{-4}	3.4	3.5
5×10^{-4}	10^{-4}	5.4	2.3
3.3×10^{-4}	10^{-4}	8.2	2.3
2.5×10^{-4}	10^{-4}	10.5	2.4
5×10^{-4}	2.5×10^{-5}	47.2	2.2
$K_1 \times 10^{-3}$ (average)		2.6	

TABLE X

STABILITY CONSTANTS FOR THE 1:1 NICKEL(II) MUREXIDE
 IN 50% ETHANOL AQUEOUS SOLUTION AT $\lambda = 460$ nm
 TEMPERATURE = 25°C, IONIC STRENGTH = 0.1 M AND pH = 5

$[\text{Ni}^{+2}]$ (M)	$[\text{H}_2\text{L}^-]$ (M)	Transmittance %	$K_1 \times 10^{-4}$
10^{-3}	2.5×10^{-5}	40.6	(dropped) 1.40
5×10^{-4}	2.5×10^{-5}	42.5	1.28
3×10^{-4}	2.5×10^{-5}	45.8	1.04
2×10^{-4}	2.5×10^{-5}	48.6	1.07
4×10^{-4}	5.0×10^{-5}	20.2	0.97
$K_1 \times 10^{-4}$ (average)			1.10

TABLE XI

STABILITY CONSTANTS FOR THE 1:1 HOLMIUM(III) MUREXIDE
 IN 50% AQUEOUS ETHANOL SOLUTION AT $\lambda = 470$ nm,
 TEMPERATURE = 12°C, IONIC STRENGTH = 0.1 M AND pH = 5

$[Ho^{+3}](M)$	$[H_2L^{-}](M)$	Transmittance%	$K_1 \times 10^{-4}$
2.5×10^{-5}	0.5×10^{-5}	86.6	(dropped) 4.4
5.0×10^{-5}	0.5×10^{-5}	84.5	2.4
7.5×10^{-5}	0.5×10^{-5}	82.6	3.0
2.5×10^{-5}	0.75×10^{-5}	81.0	2.4
5.0×10^{-5}	0.75×10^{-5}	77.0	2.9
7.5×10^{-5}	0.75×10^{-5}	74.8	2.9
$K_1 \times 10^{-4}$ (average)		$2.7 \pm (9.5\%)$	

TABLE XII

STABILITY CONSTANTS FOR THE 1:1 DYSPROSIUM(III) MUREXIDE
 IN 50% AQUEOUS ETHANOL SOLUTION AT $\lambda = 470$ nm,
 TEMPERATURE = 12°C, IONIC STRENGTH = 0.1 M AND pH = 5

$[\text{Dy}^{+3}](\text{M}) \times 10^5$	$[\text{H}_2\text{L}^-](\text{M}) \times 10^5$	Transmittance%	$K_1 \times 10^{-4}$
2.5	0.5	86	3.3
5.0	0.5	84	2.9
7.5	0.5	82.2	3.3
2.5	0.75	79.6	3.5
5.0	0.75	75.8	3.8
7.5	0.75	75.2	2.9
$K_1 \times 10^{-4}$ (average)		3.3 ($\pm 9.7\%$)	

TABLE XIII

STABILITY CONSTANT FOR THE 1:1 TERBIUM(III) MUREXIDE
 IN 50% AQUEOUS ETHANOL SOLUTION AT $\lambda = 470$ nm,
 TEMPERATURE = 12°C, IONIC STRENGTH = 0.1 M AND pH = 5

$[\text{Tb}^{+3}] \times 10^{+5}$ (M)	$[\text{H}_2\text{L}^-] \times 10^{+5}$ (M)	Transmittance %	$K_1 \times 10^{-4}$
2.5	0.5	85	4.8
5.0	0.5	82.3	5.3
7.5	0.5	82.3 (dropped)	3.5
2.5	0.75	78.5	4.6
5.0	0.75	75	4.9
7.5	0.75	74	4.2
$K_1 \times 10^{-4}$ (average)		4.8 ($\pm 7.5\%$)	

TABLE XIV

STABILITY CONSTANT FOR THE 1:1 GADOLIMIUM(III) MUREXIDE
 IN 50% AQUEOUS ETHANOL SOLUTION AT $\lambda = 470$ nm,
 TEMPERATURE = 12°C, IONIC STRENGTH = 0.1 M AND pH = 5

$[\text{Gd}^{+3}] \times 10^5$ (M)	$[\text{H}_2\text{L}^-] \times 10^5$ (M)	Transmittance%	$K_1 \times 10^{-4}$
2.5	0.5	84	8.3
5.0	0.5	82.3	8.0
7.5	0.5	81 (dropped)	12.4
2.5	0.75	77.6	7.7
5.0	0.75	74.8	8.0
7.5	0.75	73.5	8.5
$K_1 \times 10^{-4}$ (average)		8.1	

TABLE XV

STABILITY CONSTANT FOR THE 1:1 SAMARIUM(III) MUREXIDE
 IN 50% AQUEOUS ETHANOL SOLUTION AT $\lambda = 470$ nm,
 TEMPERATURE = 12°C, IONIC STRENGTH = 0.1 M AND pH = 5

$[\text{Sm}^{+3}] \times 10^5$ (M)	$[\text{H}_2\text{L}^-] \times 10^5$ (M)	Transmittance %	$K_1 \times 10^{-5}$
1.25	0.375	88.6	1.1
2.50	0.375	87.3	1.0
3.75	0.375	86.4	0.98
5.00	0.625	76.9	1.4
6.25	0.625	76.6	0.93
K_1 (average)		1.1×10^5	

TABLE XVI

STABILITY CONSTANT FOR THE 1:1 EUROPIUM(III) MUREXIDE
 IN 50% AQUEOUS ETHANOL SOLUTION AT $\lambda = 470 \text{ nm}$,
 TEMPERATURE = 12°C , IONIC STRENGTH = 0.1 M AND pH = 5

$[\text{Eu}^{+3}] \times 10^5 \text{ (M)}$	$[\text{H}_2\text{L}^-] \times 10^5 \text{ (M)}$	Transmittance %	$K_1 \times 10^{-5}$
1.25	0.375	88.7	1.1
2.50	0.375	86.9	1.1
3.75	0.375	86.2	1.1
5.00	0.375	85.4	1.34
K_1 (average)		1.2×10^5	

$$\frac{d \ln K_1}{dt} = \frac{\Delta H^\circ}{RT^2} \quad (\text{IV-6})$$

$$\Delta S^\circ = \frac{\Delta H^\circ + RT \ln K_1}{T} \quad (\text{IV-7})$$

For water solution, ΔH° is -1.6 ± 0.3 kcal/mole and ΔS° is 9.4 ± 1 e.u. For 50% aqueous DMSO solution, ΔH° is -5.6 ± 0.5 kcal/mole and ΔS° is -0.3 ± 1.5 e.u. The decrease in the stability constant with increasing temperature is less for the water system than that for the 50% aqueous DMSO system.

The sign and magnitude of the ΔS° for nickel(II) murexide in aqueous solution is consistent with the so called "chelate effect", since three water molecules coordinated to the Ni (II) have been replaced by one free ligand and thus a positive value of ΔS° is expected on the grounds of a net increase in the total number of free molecules. The effect is not seen in the aqueous DMSO system which has a small and negative value of ΔS° . The increased stability constant for nickel murexide in aqueous DMSO solution compared to that in water is due to a more negative enthalpy change for the complexation reaction. In order to elucidate the solvent effect on the stability constant, some properties of DMSO and water mixtures should be examined. During the past several years, nuclear magnetic resonance spectrometry has been used to determine the primary coordination numbers and solvent exchange rates of metal ions in nonaqueous solvents (48-52). The relative

solvation of metal ions in a mixed solvent system has also been subjected to intensive research recently (53-55). In an H_2O - DMSO Al (III) system, the average number of DMSO molecules (\bar{n}) bound to each aluminum(III) versus the molar ratio of free DMSO to free water has been obtained (56). This work indicates DMSO is a relatively good coordinating agent, however for a 50% by volume H_2O - DMSO mixture which has a molar ratio of 0.23, the primary sphere of the aluminum(III) is still a layer of water molecules. Similar studies have been made for chromium(III) (57) but not for nickel(II). The larger stability constant for nickel(II) murexide in the H_2O - DMSO solvent system is brought about primarily by the strong interaction between the bulk H_2O and DMSO molecules rather than by the difference in the solvation of the various ionic species in the solution or by the difference in the dielectric property of the mixture.

Porter and Brey (58) have reported that a pyrrole monomer complexes with DMSO solvent molecules with a hydrogen bond strength of 3.0 kcal/mole. Ting, et. al., (59) have reported that, in very dilute solutions of H_2O in DMSO, in the region $(H_2O)/(DMSO) < 0.04$ (molar ratio), the water is a monomer which is hydrogen bonded by two DMSO molecules. In the preparation of mixed solvents, when equal volumes of DMSO and H_2O are mixed, the temperature increases about $20^\circ C$ and an appreciable (a few percentage of the total initial volume) volume shrinkage occurs. All these indicate that there is a strong solvent-solvent interaction between DMSO and H_2O . If the mixed solvents exist in a partially

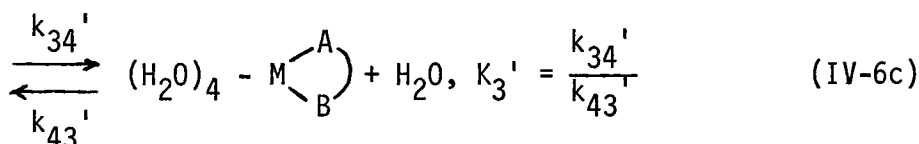
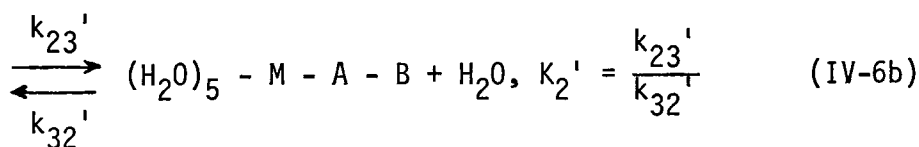
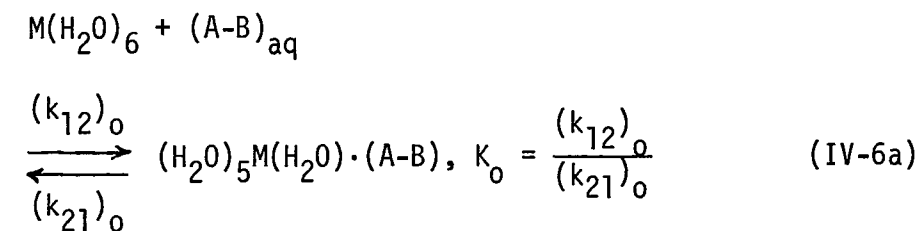
frozen state because of strong intermolecular forces or hydrogen bonding etc., it is understandable that the enthalpy and entropy changes of metal ligand complexation in such a solvent system will result in more negative values compared to those in a less frozen solvent state. This is because the formation of the complex will be accompanied by loss of solvent molecules in the hydration sphere and the strong interaction between the dissociated solvent molecules and bulk solvent will result in a large negative enthalpy and entropy contributions to the complex formation reaction.

In a 50% aqueous ethanol system, the increase in stability constant is due to a decrease in dielectric constant and polarity of the bulk solution compared to those in aqueous solution. Consequently, a positive ΔS° is responsible for a more negative change of ΔG° (60). In general, it is difficult to predict the solvating ability of a solvent toward a cation or anion. Many factors such as structural features of solvents, microscopic dielectric constant, and ion-solvent or solvent-solvent interactions are not yet clearly defined.

2. Kinetics Studies

a) Nickel(II) Murexide Complex Formation

The generally accepted mechanism for complex formation between the metal ion and a bidentate ligand A-B, is a multiple step system proposed by Eigen (79) and extended by Hammes (20). This mechanism is represented by the equations



where M represents metal ion and A-B represents two binding sites of the attacking ligand. Charges on the ions have been neglected for convenience.

The first reaction is the formation of an ion pair, which consists of two discrete steps. One step is the diffusion controlled approach of the two hydrated ions to form an ion-associate in which the ions are separated by the strongly bonded water molecules of the inner hydration sphere. The second step involves the loss of a water molecule between the ions which were originally associated with the anion. The latter step is slightly slower than the first. These two discrete steps correspond to A and B in Figure 1. The next step involves the loss of a water molecule from the inner hydration sphere of the metal ion and the formation of the metal ligand bond. The final step is the formation of the second metal ligand bond to form the fully chelated species.

The rate of formation of metal complex in terms of the above mechanism can be expressed by

$$\frac{d[(H_2O)_4M \begin{array}{c} \curvearrowright A \\ \curvearrowleft B \end{array}]}{dt} = k_{34}' [(H_2O)_5M-A-B] - k_{43}' [(H_2O)_4M \begin{array}{c} \curvearrowright A \\ \curvearrowleft B \end{array}] \quad (IV-7)$$

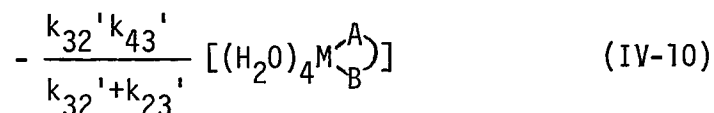
With the assumption of a steady state system for $[(H_2O)_5M-A-B]$, that is to say $\frac{d[(H_2O)_5M-A-B]}{dt} = 0$, the equation becomes

$$\frac{d[(H_2O)_4M \begin{array}{c} \curvearrowright A \\ \curvearrowleft B \end{array}]}{dt} = \frac{k_{23}' k_{34}'}{k_{32}' + k_{34}'} [(H_2O)_5M(H_2O)(A-B)] - \frac{k_{32}' k_{43}'}{k_{32}' + k_{34}'} [(H_2O)_4M \begin{array}{c} \curvearrowright A \\ \curvearrowleft B \end{array}] \quad (IV-8)$$

If the first step is very fast with respect to the second and third step, then the first step can be assumed to be at equilibrium at all times in the course of reaction

$$K_0 = \frac{[(H_2O)_5M(H_2O)(A-B)]}{[M(H_2O)_6][A-B]_{aq}} \quad (IV-9)$$

$$\frac{d[(H_2O)_4M \begin{array}{c} \curvearrowright A \\ \curvearrowleft B \end{array}]}{dt} = \frac{K_0 k_{23}' k_{34}'}{k_{32}' + k_{34}'} [M(H_2O)_6][A-B]_{aq}$$



Therefore, the rate constants for the formation and dissociation of bidentate complex may be represented by the following equations respectively.

$$k_{1f} = \frac{K_0 k_{23}' k_{34}'}{k_{32}' + k_{34}'} \quad (IV-11)$$

$$k_{1r} = \frac{k_{32}' k_{43}'}{k_{32}' + k_{34}'} \quad (IV-12)$$

According to Kustin and coworkers (6,21), two mechanisms have been derived from the above two equations. Limiting case (A) is defined when $k_{34}' \gg k_{32}'$; we have $k_{1f} = K_0 k_{23}'$ and $k_{1r} = \frac{k_{32}'}{K_3'}$, that is, the overall rate of complex formation is determined by the rate of expulsion of the first water molecule from the inner hydration sphere and the overall rate of dissociation is related to the rate of dissociation of metal-ligand bond. Most of the published results of ligand substitution reactions are in good agreement with this assumption (61), and this mechanism is classified as normal substitution reaction. By using the relationship $k_{1f} = K_0 k_{23}'$, we have

$$\Delta H_f^* = \frac{d \ln k_{1f}}{dT} = \frac{d \ln K_0}{dT} + \frac{d \ln k_{23}'}{dT} = \Delta H_0 + \Delta H_{23}^* \quad (IV-13)$$

where ΔH_f^* is the activation enthalpy change for the overall process, ΔH_0 is the thermodynamic enthalpy change for the ion pair formation. ΔH_{23}^* is the activation enthalpy for the expulsion of the first water molecule. Limiting case (B) is defined when $k_{32}' \gg k_{34}'$; we have $k_{1f} = K_0 K_2' k_{34}'$ and $k_{1r} = k_{43}'$. This mechanism is classified as a sterically controlled mechanism. In this case the rate of the reaction depends on the nature of the ligand. The overall activation enthalpy is composed of two discrete thermodynamic enthalpy changes and one activation enthalpy change for the rate-determining step.

Between these two limiting cases we have the condition when $k_{32}' \geq k_{34}'$; we have $k_{1f} = \frac{K_0 k_{23}'}{1 + k_{32}'/k_{34}'}$. Here the forward rate constant (k_{1f}) is reduced from $K_0 k_{23}'$ by the factor indicated. A good example of this is the reaction between cobalt(II) and β -alanine which reacts one order of magnitude slower than between cobalt(II) and α -alanine.

Two contributions are responsible for making the energy barrier for ring closure of β -alanine appreciably higher than that for α -alanine. One is the result of ring strain and the other is the additional entropy loss due to forming a six-membered chelate ring rather than a five-membered ring. The detailed picture for the activating state of the third step is that the activated complex contains the atoms of the ring in correct configuration for ring closure. All that remains to be done is the formation of a bond between the pentacoordinated metal and binding site. In the study of the complexation reaction for cobalt(II) L-carnosine system (62), the rates turned out to be in the normal range.

Since the cobalt(II) complex has a seven-membered ring and the entropy loss in forming a seven-membered ring is greater than that in forming a six-membered ring, the results of normal rates have been taken as evidence that the ligand entropy contribution to steric effects is considerably less significant than the ring strain contribution.

Recently, an abnormal reaction rate between nickel(II) and ligands having peptide linkages has been reported. The rates for the reactions between cobalt(II) and these ligands are normal, while for nickel(II) they are slow compared to other measured rates. Selected complexation rate constants for cobalt(II) and nickel(II) taken from reference 21 are shown in Table XVII. In this table, k_{1f} , k_{2f} and k_{3f} represent the respective forward rate constant for the mono-, bis-, and tris-complex formation reactions. For the cobalt(II) series it is seen that k_{1f} decreases slightly from negatively charged ligands to neutral ligands and has similar values for the same charge type of the ligands. This kind of variation is expected from the relationship, $k_{1f} = K_0 k_{23}'$. For the nickel(II) system, a similar variation was not observed. It has been suggested that the carboxylate bonding in the metal complex formation is exhibited only in the cobalt(II) system but not in the nickel (II) system where a metal-peptide chelation is reported (63).

In light of the above discussion, the detailed kinetics of nickel(II) murexide complexation formation has been studied. This system was chosen because the forward rate constant (k_{1f}) reported for cobalt(II) murexide is normal while that for nickel(II) is smaller than expected (24).

TABLE XVII

SELECTED COMPLEXATION RATE CONSTANTS FOR COBALT(II) AND NICKEL(II)

Ligand	Charge of attacking form	k_{1f}	k_{2f}	k_{3f}
Cobalt(II)				
L-Glycine	-1	1.5×10^6	2.0×10^6	8.0×10^5
Malonic acid	-1	7×10^5		
α -Alanine	-1	6.0×10^5	8.0×10^5	9.0×10^4
Glycylsarcosine	-1	4.6×10^5	8.0×10^5	
L-Carnosine	-1	4.2×10^5		
Triglycine	-1	3.1×10^5	1.0×10^5	
Tetraglycine	-1	2.6×10^5	2.3×10^5	
Glycylglycine	-1	2.0×10^5	1.6×10^5	
L-Arginine	0	1.5×10^5	8.7×10^5	2.0×10^5
1,10-Phenanthroline	0	1.4×10^5		
Imidazole	0	1.3×10^5	1.1×10^5	
Ammonia	0	9.5×10^4		
Nickel(II)				
L-Glycine	-1	4.1×10^4	5.6×10^4	4.3×10^4
α -Alanine	-1	2.0×10^4	4.0×10^4	
Oxalic acid	-1	5×10^3		
Imidazole	0	5.0×10^3	4.3×10^3	
1,10-Phenanthroline	0	3.9×10^3		
Ammonia	0	3.3×10^3		
Glycylglycine	-1	3.2×10^3	9.2×10^3	4.0×10^3
Malonic acid	-1	3.1×10^3		
L-Arginine	0	2.3×10^3	2.4×10^4	3.5×10^4
Glycylsarcosine	-1	2.0×10^3	8.0×10^3	
Tetraglycine	-1	1.8×10^3	4.9×10^3	
Triglycine	-1	1.7×10^3	5.5×10^3	

By measuring the relaxation times for different concentrations at four different temperatures, k_{1f} was calculated and is summarized in Table XVIII.

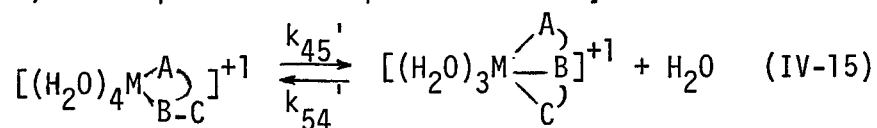
The k_{1f} values were estimated from

$$\frac{1}{\tau} = k_{1f}(\bar{C}_{N_i} + 2\bar{C}_{HL^-}) + \frac{k_{1f}}{K_1} \quad (\text{IV-14})$$

where K_1 is the usual stability constant for monocomplex formation and $k_{1r} = \frac{k_{1f}}{K_1}$.

From the fact that all of the solutions exhibited one relaxation time and the values of k_{1f} evaluated from Equation (IV-14) are practically the same at a given temperature, it is possible to propose a combined single step relaxation process for the nickel murexide system.

For a tridentate ligand, an additional step should be added to Equation (IV-6) to complete the complex formation, or



where A-B-C represents the three binding sites for the perchlorate ion. There are three steps preceding Equation (IV-15) as shown in equation (IV-6). If the intermediates $[(H_2O)_5-M-A-B-C]^{+1}$ and $[(H_2O)_4M \begin{matrix} \nearrow A \\ \searrow B \\ \quad C \end{matrix}]^{+1}$ are assumed to be in a steady state the rates of formation and dissociation are obtained by combining the various steps into a single step and they are given by

TABLE XVIII
RELAXATION TIMES AND k_{1f} FOR NICKEL(II) MUREXIDE IN AQUEOUS SOLUTION
AT IONIC STRENGTH = 0.1 M, pH = 5, AND $\lambda_{\max} = 460$ nm

$C_{Ni^{+2}}$ (M)	C_{HL^-} (M)	τ (msec)	Temp($^{\circ}$ C)	$(\bar{C}_{Ni^{+2}} + \bar{C}_{HL^-})$ (M)	k_{1f} ($M^{-1} sec^{-1}$)
0.9×10^{-3}	1×10^{-4}	547	18.0	8.7×10^{-4}	1.2×10^3
1.5×10^{-3}	1×10^{-4}	386	21.0	1.5×10^{-3}	1.3×10^3
1.0×10^{-3}	1×10^{-4}	400	21.0	1.0×10^{-3}	1.7×10^3
0.6×10^{-3}	1×10^{-4}	503	21.0	0.6×10^{-3}	1.6×10^3
2.0×10^{-3}	1×10^{-4}	110	31.5	1.95×10^{-3}	3.5×10^{-3}
1.0×10^{-3}	1×10^{-4}	171	31.5	1.0×10^{-3}	$3.5 \times 10^{+3}$
0.6×10^{-3}	1×10^{-4}	249	31.5	0.61×10^{-3}	$3.1 \times 10^{+3}$
3.3×10^{-4}	1×10^{-4}	307	31.5	0.33×10^{-3}	$3.2 \times 10^{+3}$
1.0×10^{-3}	1×10^{-4}	125	40.0	1.0×10^{-3}	$3.4 \times 10^{+3}$
0.6×10^{-3}	1×10^{-4}	140	40.0	0.61×10^{-3}	3.9×10^3

$C_{Ni^{+2}}$ = initial concentration of $NiCl_2$
 C_{HL^-} = initial concentration of Murexide
 $\bar{C}_{Ni^{+2}}$ = equilibrium concentration of Ni^{+2}
 \bar{C}_{HL^-} = equilibrium concentration of HL^-

$$k_{1f} = \frac{K_0 k_{23}' k_{34}' k_{45}'}{k_{32}' k_{43}' + k_{34}' k_{45}' + k_{32}' k_{45}'} \quad (\text{IV-16a})$$

$$k_{1r} = \frac{k_{32}' k_{43}' k_{54}'}{k_{32}' k_{43}' + k_{34}' k_{45}' + k_{32}' k_{45}'} \quad (\text{IV-16b})$$

Here the value of $K_0 k_{23}'$ is reduced to k_{1f} by a factor

$$\frac{1}{1 + \frac{k_{32}'}{k_{34}'} + \frac{k_{32}'}{k_3' k_{45}'}}$$

The reasoning for the sterically controlled reaction cannot be applied to the nickel(II) system because no steric effect was found for the reaction between cobalt(II) and murexide. In other words, the activation energy needed for a cobalt(II) monodentate substitution reaction is less than that for a nickel(II) monodentate substitution reaction. Therefore, if an additional appreciable activation energy is required in forming a chelate complex, the steric hindrance which depends only on the ligand should affect the cobalt(II) system more than the nickel(II) system (64).

If both nickel(II) and cobalt(II) react with the same bidentate ligand which is not sterically hindered in forming the chelates, the relationship, $k_{32}' \geq k_{34}'$, still holds for both as long as the rate of dissociation of the monodentate intermediate is faster than or equal to that of bidentate formation. In the case of cobalt(II) murexide, k_{1f}

will be equal to $K_0 k_{23}'$ if k_{34}' and k_{45}' are much larger than k_{32}' and k_{43}' respectively. While for the nickel system with $k_{1f} = 1.5 \times 10^3 \text{ M}^{-1} \text{ sec.}^{-1}$ at 21°C , it is evident that the factor,

$$\frac{1}{1 + \frac{k_{32}'}{k_{34}'} + \frac{k_{32}'}{K_3' k_{45}'}} = \gamma$$

is larger than one, since the normal k_{1f} value for other nickel(II) systems is around $1 \times 10^4 \text{ M}^{-1} \text{ sec.}^{-1}$. It is difficult to estimate the values for k_{34}' and k_{45}' , however, as indicated in Table XVIII, because k_{1f} and k_{2f} have values of the same order of magnitude. This implies that the negative charge of the coordinated ligand will not significantly affect the rate of the dissociation of the remaining coordinated water molecules. In general, the hypothesis that the rate of water substitution increases as the metal complex charge decreases is not true in most cases (67). Therefore, it is reasonable to assume that the value for k_{23}' , k_{34}' and k_{45}' of the cobalt(II) substitution reaction are one order of magnitude greater than those for the nickel(II) substitution reaction, since it has been determined that the rate (k_{23}') of releasing the first water molecule from the inner sphere of the cobalt(II) ion is one order of magnitude greater than that of the nickel(II) ion.

As far as the rates of step-wise dissociation are concerned, the perchlorate ion has four resonance structures, and comparing to other nickel(II) polydentate systems in aqueous solution, the relatively small value of the stability constant for nickel(II) murexide in aqueous

solution primarily results from a large positive entropy change rather than a large negative enthalpy change. Since the formation of metal ligand bonds will destroy the resonance structures of the ligand and the enthalpy change is a measurement of metal ligand bond strength, it is reasonable to assume that the metal ligand bonds are relatively weak, that is to say, the values for some of the step-wise reverse rate constants might be comparable to the values of step-wise chelate formation rate constants. Therefore, the value of the factor, γ , is larger than one and the rate, k_{1f} , is lower than the normal value. A lower substitution rate was not observed for the cobalt(II) murexide formation reaction. This is probably because the cobalt(II) ion is more labile. As illustrated above, the cobalt(II) ion has higher values for the step-wise chelation formation rate constants. Thus, the step-wise reverse rate constants might not exceed the step-wise forward rate constants. Namely, the relationship $k_{1f} = K_0 k_{23}'$ is applicable to the cobalt system but not to the nickel system.

Values of Arrhenius energies of activation for the reaction process of the system have been calculated from the slopes of the plot of $\log k_{1f}$ against $\frac{1}{\text{Temp}} \times 1000$. The entropies of activation, ΔS_f^* , enthalpies of activation, ΔH_f^* , and free energy of activation, ΔG_f^* , were obtained from the equations

$$\Delta H_f^* = \Delta E_f - RT \quad (\text{IV-17})$$

$$\ln A = \ln \frac{eRT}{Nh} + \frac{\Delta S_f^*}{R} \quad (\text{IV-18})$$

$$\Delta G_f^* = \Delta H_f^* - T\Delta S_f^* \quad (\text{IV-19})$$

where $\ln A$ is the intercept obtained from the Arrhenius plot. The uncertainties in ΔE_f and ΔS_f^* for nickel system are about ± 0.7 kcal/mole⁻¹ and ± 2.2 cal deg⁻¹ mole⁻¹ respectively.

In the calculation of ΔH_0 and ΔS_0 of ion pair formation, ΔS_0 was assumed to be equal to $-19.4 \frac{Z_- Z_+}{a}$ (66,65) with a , the distance of closest approach of the ion pair partners, equal to 5 \AA and Z_- and Z_+ are the charges on the ions.

The enthalpy change for the first step was obtained from the relationship.

$$\Delta H_0 = -RT \ln K_0 + T\Delta S_0 \quad (\text{IV-20})$$

The other parameters are defined by:

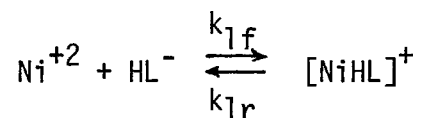
$$\Delta H^* = \Delta H_f^* - \Delta H_0 \quad (\text{IV-21})$$

$$\Delta S^* = \Delta S_f^* - \Delta S_0 \quad (\text{IV-22})$$

The results of the measured and calculated kinetic parameters are summarized in Table XIX. In this table ΔH^* and ΔS^* are the activation parameters after the correction for the rapid preequilibrium step has been made.

TABLE XIX

KINETIC DATA FOR THE NICKEL(II) MUREXIDE
FORMATION AT 20°C AND IONIC STRENGTH = 0.1 M



$K_1 = \frac{k_{1f}}{k_{1r}}$	1.65×10^3
$k_{1f}(\text{M}^{-1}\text{sec}^{-1})$	1.4×10^3
$k_{1r}(\text{sec}^{-1})$	0.85
$\Delta E_f(\text{kcal M}^{-1})$	12.5
$\Delta H_f^*(\text{kcal M}^{-1})$	11.9
$\Delta S_f^*(\text{cal deg}^{-1}\text{M}^{-1})$	-3.6
$\Delta G_f^*(\text{kcal M}^{-1})$	13
K_o	2
$k = \frac{k_{1f}}{K_o} (\text{sec}^{-1})$	0.7×10^3
$\Delta G_o(\text{kcal M}^{-1})$	-0.4
$\Delta S_o(\text{cal deg}^{-1}\text{M}^{-1})$	7.8
$\Delta H_o(\text{kcal M}^{-1})$	1.9
$\Delta H^*(\text{kcal M}^{-1})$	10
$\Delta S^*(\text{cal deg}^{-1}\text{M}^{-1})$	-10.4

For the nickel(II) bioxalate reaction, the values of the activation parameters have previously been obtained (79). For this system, ΔE_f is 15 kcal mole⁻¹ and ΔS_f^* is 7 cal deg⁻¹ mole⁻¹. Comparing these values to those obtained for the nickel(II) murexide system, the latter is found to have a lower ΔE_f (12.5 kcal mole⁻¹) and ΔS_f^* (-3.6 cal deg⁻¹ mole⁻¹). This may indicate the absence of a steric effect in the nickel murexide complexation reaction, if a higher ΔE_f value is considered to be the primary indicator of the existence of a steric effect.

In the study of solvation effects on the rates of fast reactions in solution, a collection of rate parameters for solvent exchange reactions and Dq values in various solvents for nickel(II) and cobalt(II) systems has been obtained and is shown in Table XX (16,17). From this table, it is seen that the Dq value for CH₃OH, DMF and DMSO are all lower than that of water, yet ΔH^* for water exchange is lower than for the other three solvents. The ΔH^* value is apparently not only a function of Dq value but also a function of differences in solvation between activated and ground states. The kinetics of ion association of manganese(II) sulfate in water, dioxane - H₂O and methanol - H₂O mixtures has been studied by Atkison and Kor (14). They found that the step-wise rate constants of Eigen's multiple step mechanism vary very slightly with the solvent. In the present study, the rate constants have been obtained for nickel(II) murexide in 25% DMSO, 50% DMSO - H₂O and 50% ethanol - H₂O mixtures. The k_{1f} values computed from Equation (IV-14) are summarized in Table XXI. The activation parameters obtained for 50% DMSO - H₂O mixture are almost

TABLE XX

SOLVENT - EXCHANGE RATE PARAMETERS AND Dq VALUES
FOR NICKEL(II) AND COBALT(II) SYSTEMS

Solvent	ΔH^* (kcal mole ⁻¹)	Ni(II) ΔS^* (e.u.)	Dq (cm ⁻¹)	ΔH^* (kcal mole ⁻¹)	Co(II) ΔS^* (e.u.)	Dq (cm ⁻¹)
H ₂ O	11.0	0.6	870	8.0	-4.1	861
CH ₃ OH	15.8	8.0	837	13.8	7.2	875
DMF	15.0	8.0	812	13.6	12.6	880
CH ₃ CN	10.9	-8.8	1104	8.1	-7.5	1100
DMSO	12.1	-1.3	773	-	-	-
NH ₃	11.0	2.0	1095	11.2	10.2	1080

TABLE XXI

RELAXATION TIMES AND k_{1f} FOR THE NICKEL(II) MUREXIDE FORMATION IN VARIOUS SOLVENT SYSTEMS
 IONIC STRENGTH = 0.1 M, pH ~ 5, λ_{\max} = 460 nm

$C_{Ni^{+2}}$ (M)	C_{HL^-} (M)	τ (msec)	Temp ($^{\circ}$ C)	$(\bar{C}_{Ni} + \bar{C}_{HL^-})$ (M)	k_{1f} ($M^{-1}sec^{-1}$)	Solvents
2×10^{-3}	1×10^{-4}	108	31.5	1.94×10^{-3}	3.8×10^3	25% DMSO-H ₂ O
1×10^{-3}	1×10^{-4}	184	31.5	0.96×10^{-3}	3.8×10^3	"
8×10^{-4}	1×10^{-4}	223	31.5	0.77×10^{-3}	3.6×10^3	"
6×10^{-4}	1×10^{-4}	259	31.5	0.59×10^{-3}	3.7×10^3	"
3.3×10^{-4}	1×10^{-4}	339	31.5	0.36×10^{-3}	3.6×10^3	"
6.5×10^{-4}	6×10^{-5}	378	23	0.61×10^{-3}	3.8×10^3	50% DMSO-H ₂ O
5.0×10^{-4}	5×10^{-5}	413	23	0.47×10^{-3}	4.2×10^3	"
1×10^{-3}	10^{-4}	164	31.5	0.92×10^{-3}	5.9×10^3	"
8×10^{-4}	7×10^{-5}	181	31.5	0.75×10^{-3}	6.3×10^3	"
6.5×10^{-4}	6×10^{-5}	262	31.5	0.61×10^{-3}	5.2×10^3	"
5×10^{-4}	5×10^{-5}	320	31.5	0.47×10^{-3}	5.3×10^3	"
4×10^{-4}	4.5×10^{-5}	343	31.5	0.38×10^{-3}	5.8×10^3	"
6.5×10^{-4}	6×10^{-5}	172	37	0.6×10^{-3}	8.1×10^3	"
5×10^{-4}	5×10^{-5}	178	37	0.47×10^{-3}	9.5×10^3	"
6.5×10^{-4}	6×10^{-5}	106	40	0.6×10^{-3}	12.5×10^3	"
5×10^{-4}	5×10^{-5}	134	40	0.47×10^{-3}	11.9×10^3	"
4×10^{-4}	5×10^{-5}	238	25	0.37×10^{-3}	8.4×10^3	50% ethanol-H ₂ O
3×10^{-4}	5×10^{-5}	278	25	0.28×10^{-3}	9.8×10^3	"
2×10^{-4}	5×10^{-5}	397	25	0.19×10^{-3}	9×10^3	"

∞

$C_{Ni^{+2}}$ = initial concentration of NiCl₂; C_{HL^-} = initial concentration of Murexide; $\bar{C}_{Ni^{+2}} + \bar{C}_{HL^-}$ = equilibrium concentration of Ni⁺² + HL⁻

identical to those obtained for the H₂O system. ΔE_f is 12.4 ± 0.8 kcal mole⁻¹ and ΔS_f^* is -2.4 ± 2.6 e.u. Extrapolating to the same temperature (Table XXII), k_{1f} for 50% H₂O - ethanol mixture is the highest, whereas the k_{1r} for 50% DMSO - H₂O mixture is the lowest among the four solvent systems. Compared to the water system, the increased stability constant for 50% DMSO - H₂O system is caused by the slower reverse reaction and faster forward reaction, whereas for 50% ethanol - H₂O mixture the stability constant is increased primarily due to the faster forward reaction. The variation of the forward rate constants in different solutions is roughly proportional to that of ion pair formation constants which increase with a decrease in the bulk dielectric constant of the solutions.

The activation parameters (ΔH_r^* , ΔS_r^*) for the reverse reactions may be computed from $\Delta H^\circ = \Delta H_f^* - \Delta H_r^*$ and $\Delta S^\circ = \Delta S_f^* - \Delta S_r^*$, ΔH° and ΔS° are the thermodynamic parameters for the complex formation reaction. For the water system, ΔH_r^* and ΔS_r^* are 13.5 kcal mole⁻¹ and -13 e.u., for the 50% DMSO - H₂O mixture they are 17.4 kcal mole⁻¹ and -2.1 e.u. respectively. These values indicate that the H₂O - DMSO solution has a highly ordered solvent structure, since higher ΔH_r^* rather than lower ΔS_r^* is responsible for the slow reverse reaction compared to the H₂O system. This idea can easily be understood, if, in the ionization process, the entropy decrease in going from the ground state (complex) to the activated state (partially ionized complex) can be related to the freezing of solvent molecules around the incipient ions

TABLE XXII
 THE k_{1f} AND k_{1r} VALUES EXTRAPOLATED TO 25°C
 FOR THE NICKEL(II) MUREXIDE FORMATION IN
 VARIOUS SOLVENT SYSTEMS AT IONIC STRENGTH = 0.1 M

Solvent System	$k_{1f}(\text{sec}^{-1}\text{M}^{-1})$	$k_{1r}(\text{sec}^{-1})$	$K_1 = \frac{k_{1f}}{k_{1r}}$
H ₂ O	1.8×10^3	1.15	1.57×10^3
25% DMSO - H ₂ O*	3.7×10^3	1.43	2.6×10^3
50% DMSO - H ₂ O	4.2×10^3	0.43	9.8×10^3
50% Ethanol - H ₂ O	9.0×10^3	0.83	1.1×10^4

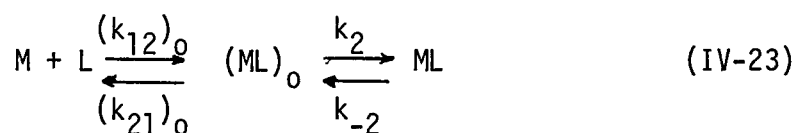
*Temperature at 31.5°C

b) Lanthanide Murexide Complex Formation

During the past several years, relaxation and N.M.R. techniques have been used to study the association and dissociation reactions for the lanthanide ions (24-29, 68-69). Not only different substitution rates but different variations with respect to the ionic size have been observed. The only common point established from these studies is that the lanthanides have a coordination number greater than six in their aquo complexes. In an attempt to explain the differences among these results, several selected papers are examined and the lanthanide murexide substitution reactions in 50% ethanol - H₂O have been studied.

The kinetics of aqueous lanthanide sulfate solution was studied by using the ultrasonic pulse technique (28-29). A single absorption observed for each lanthanide sulfate system was assigned to the step involving the release of a water molecule from the inner sphere of the metal ion. However, it is found that the equations employed in these papers to calculate the rate constants from the observed relaxation times seem inconsistent with the basic assumption which is required for simplifying these equations.

Consider the following reaction,



where (ML)₀ is outer sphere ion pair and ML is inner sphere complex. It has been shown that the simplified form of Equations (II-12) and

(II-13) cannot be obtained whenever $(k_{12})_0(M+L) + (k_{21})_0$ approaches or is less than $k_2 + k_{-2}$. For most substitution reactions in aqueous solution of the type M^{+2}, L^{-1} and M^{+2}, L^{-2} the theoretical value of $(k_{12})_0(M+L) + (k_{21})_0$ is much larger than (>2 orders of magnitude) $k_2 + k_{-2}$, but this is not true for the case of the lanthanide sulfate system because the value of $K_0 = \frac{(k_{12})_0}{(k_{21})_0}$ increases exponentially with the product of the charges on M and L, whereas $(k_{12})_0$ increases only proportionally with the product. Therefore, a small value of $(k_{21})_0$ compared to k_2 is observed. The theoretical values of K_0 , $(k_{12})_0$ and $(k_{21})_0$ at different ionic strengths in aqueous solution are listed in Table XXIII. Here K_0 and $(k_{12})_0$ are obtained from Fuoss' equation and the equation for diffusion controlled reaction with $a = 5.5 \text{ \AA}$ in both cases. The equivalent k_2 values for lanthanide sulfate varied from $1 \times 10^8 \text{ sec}^{-1}$ to $7 \times 10^8 \text{ sec}^{-1}$. The effectiveness of this approximation can be seen in the case of $M^{+2}SO_4^{-2}$ substitution reactions. The equivalent $(k_{21})_0$ value obtained experimentally is between $0.4 \times 10^8 \text{ sec}^{-1}$ and $5 \times 10^8 \text{ sec}^{-1}$ (14), whereas the value calculated theoretically is $4 \times 10^8 \text{ (sec}^{-1})$ with $a = 5 \text{ \AA}$ (the sum of ionic radii plus one water molecule).

If a three step mechanism is proposed for lanthanide sulfate substitution reactions as shown in Figure 1, according to reference 29, K_a has been evaluated to be 440 with $a = 8.86 \text{ \AA}$ (the sum of the ionic radii plus two water molecule diameters). Consequently, k_{12} is $3.4 \times 10^{10} \text{ M}^{-1} \text{ sec}^{-1}$ and k_{21} is $7.8 \times 10^7 \text{ sec}^{-1}$. Since k_{23} and k_{32}

TABLE XXIII

THE THEORETICAL ION PAIR CONSTANTS (K_o) AND
DIFFUSION CONTROLLED RATE CONSTANTS AT 25°C

$$(Z_1 = +3, Z_2 = -1)$$

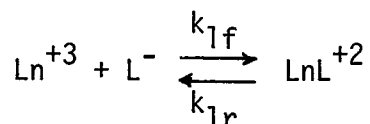
μ	K_o	$(k_{12})_o$ ($M^{-1}sec.^{-1}$)	$(k_{21})_o$ ($sec.^{-1}$)
0.20	3.7	---	---
0.10	5.2	---	---
0.05	7.5	---	---
0.00	20	2.7×10^{10}	1.3×10^9

$$(Z_1 = +3, Z_2 = -2)$$

μ	K_o	$(k_{12})_o$ ($M^{-1}sec.^{-1}$)	$(k_{21})_o$ ($sec.^{-1}$)
0.20	33	---	---
0.10	65	---	---
0.05	125	---	---
0.00	880	5.4×10^{10}	6.1×10^7

involve the desolvation and solvation of inner sphere of the anion, it is reasonable to assume that they are smaller than k_{12} and k_{21} respectively. The reported values for k_{34} varied from 1×10^8 to $7 \times 10^8 \text{sec}^{-1}$, therefore the three relaxation times corresponding to the three steps must be coupled even though only one relaxation process is observed. Hence, the results obtained from the simplified equation which relates the rate constants for the third step to the observed relaxation times could be incorrect. A similar approach has been used for the CuSO_4 substitution reaction by Petrucci and Hemmes (70).

The lanthanide-anthranilate (27) and lanthanide murexide (24) substitution reactions in aqueous solution have been studied by a temperature jump technique. The rate constants and activation parameters were obtained by assuming a single step reaction (Table XXIV)



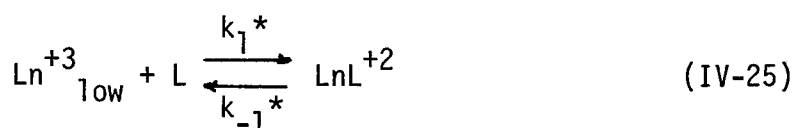
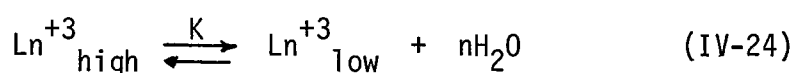
A comparison of the data shows that for the lanthanide murexide reactions the rate of complex formation in the lanthanum to europium region is about $9 \times 10^7 \text{M}^{-1} \text{sec}^{-1}$. In the europium to erbium region, the rate decreases gradually; in the erbium to lutetium region, it remains $1 \times 10^7 \text{M}^{-1} \text{sec}^{-1}$. For the lanthanide-anthranilate reactions, the rate has two peaks at Eu^{+3} and Lu^{+3} and larger values of ΔH_f^* and ΔS_f^* were observed for Gd^{+3} (f⁷) and Lu^{+3} (f¹⁴).

TABLE XXIV

SUMMARY OF KINETIC DATA FOR THE LANTHANIDE - ANTHRANILATE AND MUREXIDE SYSTEMS

	MUREXIDE	ANTHRANILATE		
	$k_{1f}(\text{M}^{-1}\text{sec}^{-1}) \times 10^{-7}$	$k_{1f}(\text{M}^{-1}\text{sec}^{-1}) \times 10^{-7}$	$\Delta H_f^*(\text{kcal/mole})$	$\Delta S_f^*(\text{e.u.})$
La	8.6	5.5	5.3	-5
Ce	9.5	--	--	-
Pr	8.6	4.6	5.1	-6
Nd	9.3	--	--	--
Sm	9.6	6.3	2.9	-13
Eu	8.2	10.5	3.3	-12
Gd	5.2	5.9	9.1	+9
Tb	3.0	3.5	--	--
Dy	1.7	1.4	4.4	-10
Ho	1.4	--	--	--
Er	1.0	5.8	3.4	-11
Tm	1.1	--	--	--
Yb	1.1	6.9	5.4	-4
Ln	1.3	9.5	9.5	+10

In order to explain the varying values of ΔH_f^* and ΔS_f^* for Gd^{+3} and Lu^{+3} as compared to other lanthanides, a mechanism was proposed by Swinehart and his coworkers. The mechanism proposes that for gadolinium and lutetium complexes, a change in coordination number from Ln^{+3}_{high} to Ln^{+3}_{low} occurs.



If reaction (IV-24) equilibrates rapidly compared to reaction (IV-25), then $k_{1f} = Kk_1^*$, $\Delta H_f^* = \Delta H_K + \Delta H_{f_1}^*$ and $\Delta S_f^* = \Delta S_K + \Delta S_{k_1}^*$. The positive enthalpy and entropy changes for the conversion of octahedral to tetrahedral complexes have been taken as evidence that ΔH_K and ΔS_K would be positive (71). Therefore, they concluded that these positive values added to the normal activation enthalpy and entropy changes for other lanthanides having only one coordinated hydration structure, account for the more positive values of ΔH_f^* and ΔS_f^* for gadolinium and lutetium.

After careful analysis of the treatment of the data for the anthranilate system, it appears that the above mechanism proposed is still inadequate. Since the equilibrium constant (K_1) was defined as;

$$K_1 = \frac{[LnL^{+2}]}{[Ln^{+3}][L^-]} = \frac{k_{1f}}{k_{1r}} \quad (IV-26)$$

where $[\text{Ln}^{+3}]$ is equal to the sum of equilibrium concentrations for $[\text{Ln}^{+3}_{\text{high}}]$ and $[\text{Ln}^{+3}_{\text{low}}]$. According to the reaction scheme (IV-24) and (IV-25) under equilibrium conditions and substituting Kk_1^* for k_{1f} , we have:

$$\frac{k_{1f}}{k_{-1}^*} = \frac{[\text{LnL}^{+2}]}{[\text{Ln}^{+3}_{\text{high}}][\text{L}^-]} \quad (\text{IV-27})$$

From the fact that the K value is unknown for this study and $[\text{Ln}^{+3}]$ has been used to calculate rate constants and activation parameters, it is obvious that the results obtained do not reflect the mechanism proposed unless $[\text{Ln}^{+3}_{\text{high}}]$ equilibrium concentration has been used. This requires a knowledge of K or if the value of $K = \frac{[\text{Ln}^{+3}_{\text{low}}]}{[\text{Ln}^{+3}_{\text{high}}]}$ is relatively small so that $[\text{Ln}^{+3}_{\text{high}}]$ is approximately equal to $[\text{Ln}^{+3}]$. If we assume K equal to $\frac{1}{10}$, then $k_{1f} = \frac{k_1^*}{10}$. Now from the observed rate constants, k_1^* should be $5.9 \times 10^8 \text{ M}^{-1} \text{ sec}^{-1}$ and $9.5 \times 10^8 \text{ M}^{-1} \text{ sec}^{-1}$ for Gd^{+3} and Ln^{+3} respectively. Apparently such high values for k_1^* compared to the other normal substitution rates (k_{1f}) cannot be satisfactorily interpreted on the basis of the above mentioned mechanism.

The lanthanide complexation in 50% ethanol - H_2O was carried out at 12°C . The relaxation times evaluated were based on the assumption that the observed relaxation spectrum consisted of a single step chemical relaxation process which was resolved according to equation (III-11). The forward rate constants (k_{1f}), with about 30% error, were

calculated from Equation (III-14) and are summarized in Table XXII together with the relaxation times observed. Statistically (72), a tridentate complex, $[M(H_2O)_{N-3n}L_n]$, has n sites from which to lose a ligand, whereas $[M(H_2O)_{N-3(n-1)}L_{n-1}]$ has $N-3(n-1)$ sites at which to gain a ligand. Thus, the relative probability of passing from $[M(H_2O)_{N-3(n-1)}L_{n-1}]$ to $[M(H_2O)_{N-3n}L_n]$ is proportional to $\frac{N-3(n-1)}{n}$. Hence, on the basis of these considerations by assuming N equal to 9 for lanthanides, the K_2 value can be estimated from the equation

$$\frac{K_2}{K_1} = \frac{ML_2}{ML} \cdot \frac{M}{ML} = \frac{1}{3}$$

From the relationship of $\frac{ML_2}{ML} = K_2[L]$, the portion of di-chelate can be neglected, since the $K_2[L]$ values are very small compared to one at the present concentrations.

The rates shown in Table XXV do not differ from those obtained for lanthanide murexide in aqueous solution, even though the theoretical K_0 value in 50% ethanol - H_2O is about three times greater than that in H_2O for these systems. Thus the result that the rate is approximately proportional to the ion pair constant for nickel substitution reactions is not observed in these reactions.

A rate constant of $6 \times 10^8 \text{ sec.}^{-1}$ for aqueous gadolinium solution was obtained from oxygen-17 N.M.R. studies of solvent exchange at 25°C . A primary coordination number of 9 was assumed for gadolinium (73). A rate constant of $6.3 \times 10^7 \text{ sec.}^{-1}$ was reported by Reuben and Fiat for the solvent exchange of dysprosium. This value was also obtained by

TABLE XXV

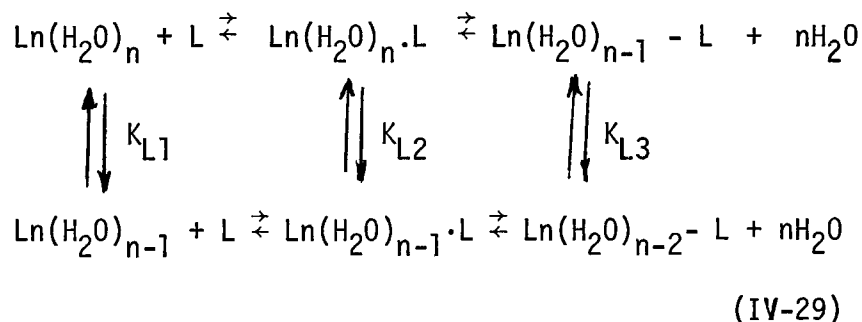
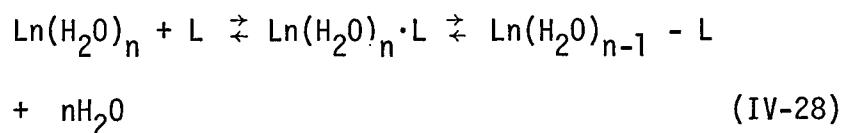
KINETIC DATA AND RATES FOR THE LANTHANIDE- MUREXIDE
SYSTEMS IN 50% ETHANOL - H₂O SOLUTION AT 12°C

$C_{H_3O^{+3}}$ M	C_{HL^-} M	pH	τ μsec	$k_{1f} \times 10^{-7}$ $M^{-1} \text{sec}^{-1}$
4×10^{-5}	2×10^{-5}	5	790	1.6
2.5×10^{-5}	1×10^{-5}	5	800	2.0
9×10^{-5}	3×10^{-5}	5	490	1.7
$C_{Dy^{+3}}$	C_{HL^-}			
4×10^{-5}	2.4×10^{-5}	5	560	2.5
3×10^{-5}	2×10^{-5}	5	770	2.1
9×10^{-5}	3×10^{-5}	5	460	2.0
$C_{Tb^{+3}}$	C_{HL^-}			
4×10^{-5}	2×10^{-5}	5	550	3.1
6×10^{-5}	2×10^{-5}	5	460	3.0
3×10^{-5}	2×10^{-5}	5	640	3.1
5×10^{-5}	2×10^{-5}	5	580	2.6
$C_{Gd^{+3}}$	C_{HL^-}			
4×10^{-5}	2×10^{-5}	5	410	5.3
2×10^{-5}	1×10^{-5}	5	590	5.4

proton magnetic resonance studies (74). The above studies are a direct measurement of solvent exchange between coordinated and bulk solvents. If there is no ligand effect for a lanthanide ligand substitution reaction, the rate-determining step will be the elimination of the first water molecule from the inner sphere of the metal ion, therefore the forward rate constant obtained for the same lanthanide ion by the solvent exchange methods and the relaxation techniques should be within a reasonable range. In fact, a one order of magnitude difference in the rates has been observed. In addition, the ligand effect which will reduce appreciably the rates of the solvent exchange reactions, the rates of substitution reactions are further complicated by the change in coordination number in the lanthanide series. Thermodynamically, it has been concluded that there is a coordination number change near the middle of the lanthanide series and for these middle rare earth ions, the two hydration structures with different coordination numbers are in equilibrium (25,75). A great deal of other data such as conductivity measurements (76), apparent molal volume at infinite dilution (77) and X-ray study of EDTA complexes (78) also support the idea of a change in coordination number. Kinetically, the effect of coordination number change on the substitution rates is still unknown.

Three questions are brought about from the results of the various lanthanide systems. One is why the rates obtained by the temperature jump technique are about one order of magnitude less than those of solvent exchange reactions obtained by N.M.R. studies for the various

systems. Another is why the variation of the rate constant as a function of ionic size changes certain points, and the third is why the ethanol - H₂O solution has no effect on the rates for the lanthanide murexide system. A purely electrostatic interaction has been used to explain the linear rate dependence with inverse cationic radius observed for the alkaline earth ions with the exception of magnesium (II). Similarly a decrease in primary coordination number for some lanthanide ions would cause an increase in the strength of the metal ion water interaction, therefore, it is suggested that the rate for the solvent exchange reaction would decrease from the lighter ions to the heavier ones with the magnitude reported from the aforementioned N.M.R. studies. Thus the smaller rates observed for the lanthanide substitution reactions are apparently due to a ligand effect. From many experimental results that solutions of the middle rare earth ions probably consist of equilibrium mixtures of species having both the higher and lower coordination numbers, the following reaction schemes are proposed.



Charges on the various species are omitted for convenience, $\text{Ln}(\text{H}_2\text{O})_n \cdot \text{L}$, represents outer sphere ion pair, $\text{Ln}(\text{H}_2\text{O})_{n-1} - \text{L}$ and $\text{Ln}(\text{H}_2\text{O})_{n-2} - \text{L}$, the final complexes. K_{L1} is defined as $\frac{\text{Ln}(\text{H}_2\text{O})_{n-1}}{\text{Ln}(\text{H}_2\text{O})_n}$, K_{L2} as $\frac{\text{Ln}(\text{H}_2\text{O})_{n-1} \cdot \text{L}}{\text{Ln}(\text{H}_2\text{O})_n \cdot \text{L}}$ and K_{L3} as $\frac{\text{Ln}(\text{H}_2\text{O})_{n-2} - \text{L}}{\text{Ln}(\text{H}_2\text{O})_{n-1} - \text{L}}$. If the ligand itself is a chelate species, one or more steps must be added to the above reaction schemes as illustrated for the nickel(II) murexide reaction. Reaction (IV-28), refers to the lanthanides having only one hydration structure whereas reaction (IV-29) refers to these having two hydration structures. For reaction (IV-29) it is seen that not only $\text{Ln}(\text{H}_2\text{O})_n$ and $\text{Ln}(\text{H}_2\text{O})_{n-1}$ but the subsequent outer and inner ion pair species are all in equilibrium with each other. These equilibrium steps should be a function of the cation as well as the ligand. For example, the K_{L1} value varies only with the cation whereas the K_{L3} varies with both the cation and ligand. This mechanism with a possible ligand effect may account for the unusual variations and the lower values of bimolecular rate constants for the various lanthanide systems. The absence of solvent effect on the rates for the lanthanide murexide substitution reactions further indicates that a combined single step rate expression as shown in Equation (IV-16a) is not adequate to describe the substitution reactions involving two hydration structures. To substantiate the idea of the above mechanism, more work on solvent exchange and monodentate substitution reaction studies are necessary. A comparison of the rate constants between the solvent exchange reactions, monodentate and polydentate substitution reactions may reveal a general mechanism for the lanthanide substitution reactions.

BIBLIOGRAPHY

1. Hammes, G. G., Science, 151, 1507 (1966).
2. Czerlinski, G. and M. Eigen, Z. Elektrochem., 63, 652 (1959).
3. Strehlow, H. and M. Becker, ibid., 63, 457 (1959).
4. Ljunggren, S and O. Lamm, Acta Chem. Scand., 12, 1834 (1958).
5. Kirschner, "Advances in the Chemistry of the Coordination Compounds," The MacMillan Company, New York (1961).
6. Kustin, K., R. F. Pasternack, and E. Weinstock, J. Amer. Chem. Soc., 88, 4610 (1966).
- 6'. Bear, J. L. and C. T. Lin, J. Phys. Chem., 72, 2026 (1968).
7. Diebler, H. and M. Eigen, Z. Physik. Chem., N. F., 20, 229 (1959).
8. Eigen, M. and K. Tamm., Z. Elektrochem., 66, 93 (1962).
9. Eigen, M. and K. Tamm., Z. Elektrochem., 66, 107 (1962).
10. Hague, D. N., "Relaxation Methods for Studying very Rapid Reactions in Solution," The Royal Institute of Chemistry, London, W. C. I., 1964.
11. Eigen, M. E. and E. M. Eyring, J. Amer. Chem. Soc., 84, 3254 (1962).
12. Porter, G., ed. "Progress in Reaction Kinetics," 2, 287 (1964).
13. Ralph, G. P. and P. Ellgen, Inorg. Chem., 6, 1379 (1967).
14. Atkinson, G. and S. K. Kor, J. Phys. Chem., 69, 128 (1965).
15. Petrucci, S. and M. Battistini, J. Phys. Chem., 71, 1181 (1967).
16. Angerman, N. S. and R. B. Jordan, Inorg. Chem., 8, 2579 (1969).
17. Babiec, J. S., Jr., C. H. Langford and T. R. Stengle, Inorg. Chem., 5, 1362 (1966).
18. Basolo, F. and R. G. Pearson, "Mechanisms of Inorganic Reactions," 2nd. ed; John Wiley and Sons, Inc., New York, N. Y., 1967, p. 145.
19. Lin, C. T. and J. L. Bear, J. Inorg. Nucl. Chem., 31, 263 (1969).
20. Hammes, G. G. and J. I. Steinfeld, J. Amer. Chem. Soc., 84, 4639 (1962).

21. Kustin, K. and R. F. Pasternack, J. Phys. Chem., 73, 1 (1969).
22. Kowalak, A., K. Kustin, R. F. Pasternack and S. Petrucci, J. Amer. Chem. Soc., 89, 3126 (1967).
23. Cassatt, J. C. and R. G. Wilkins, J. Amer. Chem. Soc., 90, 6045 (1968).
24. Geier, G., Ber Bunsenges., Physik, Chem., 69, 617 (1965).
25. Graffeo, A. J., Ph.D. Dissertation, University of Houston, Houston, Texas, 1967.
26. Silber, H. B. and J. H. Swinehart, J. Phys. Chem., 71, 4344 (1967).
27. Silber, H. B. and J. H. Swinehart, Inorg. Chem., 8, 819 (1969).
28. Purdie, N. and C. A. Vincent, Trans. Faraday Soc., 63, 2745 (1967).
29. Fay, D. P., D. Litchinsky and N. Purdie, J. Phys. Chem., 73, 544 (1969).
30. Caldin, E. F., "Fast Reactions in Solution," John Wiley and Sons, N. Y., (1964).
31. Eigen, M. and L. DeMaeyer, "Technique of Organic Chemistry," VIII, part 2, "Investigation of Rates and Mechanisms of Reactions," S. Friess, E. Lewis and A. Weissberger, eds., Interscience, New York (1963).
32. Amdur, I. and G. G. Hammes, "Chemical Kinetics: Principles and Selected Topics," McGraw-Hill Book Company, N. Y. (1966).
33. Smoluchowski, M. V., Z. Phys. Chem., 92, 129 (1917).
34. Noyes, R. M., "Progress in Reaction Kinetics," p. 137, Academic Press, 1961.
35. Schultz, R. F., Z. Phys. Chem. (Frankfurt), 8, 284 (1956).
36. Debye, P., Trans. Electrochem. Soc., 82, 265 (1942).
37. Fuoss, R. M., J. Amer. Chem. Soc., 80, 5059 (1958).
38. Eigen, M., Z. Physik. Chem. (Frankfurt), 1, 176 (1954).
39. Benson, S. W., "The Foundations of Chemical Kinetics," McGraw-Hill Book Company, New York, Toronto, London (1960).

40. Steinfeld, J. T., B.S. Thesis, Massachusetts Institute of Technology, 1962.
41. French, T. C. and G. G. Hammes, "The Temperature-Jump Method," Department of Chemistry, Massachusetts Institute of Technology and Cornell University.
42. Klotz, I. M. and W. C. L. Ming, J. Amer. Chem. Soc., 75, 4159 (1953).
43. Schwarzenbach, G., W. Biedermann, and F. Bangerter, Helv. Chim. Acta, 29, 811 (1946).
44. Schwarzenbach, G. and H. Gysling, Helv. Chim. Acta, 32, 1314, 1484 (1949).
45. Welcher, F. J., "The Analytical Uses of Ethylenediamine Tetraacetic Acid," D. Van Nostrand Company, Inc., Princeton, New Jersey (1958).
46. Martell, A. E. and M. Calvin, "Chemistry of the Metal Chelate Compounds," Prentice Hall, New York (1952).
47. Same as reference 14.
48. Matwiyoff, N. A. and H. Taube, J. Amer. Chem. Soc., 90, 2796 (1968).
49. Nakamura, S. and S. Meiboom, J. Amer. Chem. Soc., 89, 1765 (1967).
50. Matwiyoff, N. A. and W. G. Movins, J. Amer. Chem. Soc., 89, 6077 (1967).
51. Thomas S. and W. L. Reynolds, J. Chem. Phys., 44, 3148 (1966).
52. Movius, W. G. and N. A. Matwiyoff, Inorg. Chem., 6, 847 (1967).
53. Fratiello, A. and D. P. Miller, Mol. Phys., 11, 37 (1966).
54. Fratiello, A., R. E. Lee, V. M. Nishida and R. E. Schuster, J. Chem. Phys., 47, 4951 (1967).
55. Fratiello, A. and R. E. Schuster, Tetrahedron Letters, 46, 4641 (1967).
56. Olander, D. P., R. S. Marianelli and R. C. Larson, J. Anal. Chem., 41, 1097 (1969).
57. Ashley, K. R., R. E. Hamm and R. H. Magnuson, Inorg. Chem., 6, 413 (1967).

58. Porter, D. M. and W. S. Brey, Jr., J. Phys. Chem., 71, 3779 (1967).
59. Ting, S. F., S. M. Wang and N. C. Li, Can. J. Chem., 45, 425 (1967).
60. Frost, A. A. and R. G. Pearson, "Kinetics and Mechanism," John Wiley and Sons, Inc., New York, London (1953).
61. Eigen, M. and R. G. Wilkins, "Mechanisms of Inorganic Reactions," Advances in Chemistry Series, No. 49, American Chemical Society, Washington, D. C., 1965.
62. Pasternack, R. F. and K. Kustin, J. Amer. Chem. Soc., 90, 2295 (1968).
63. Freeman, H. C., Adv. Protein Chem., 22, 257 (1967).
64. Kowalak, A., K. Kustin, R. F. Pasternack, and S. Petrucci, J. Amer. Chem. Soc., 89, 3126 (1967).
65. Nancollas, G. H. and N. Sutin, Inorg. Chem., 3, 360 (1964).
66. Cavasino, F. P., J. Phys. Chem., 69, 4380 (1965).
67. Margerum, D. W. and H. M. Rosen, J. Amer. Chem. Soc., 89, 1088 (1967).
68. Marianelli, R., Ph.D. Thesis, University of California, Berkeley, California, 1966.
69. Reuben, J. and D. Fiat, Chem. Commun., 729 (1967).
70. Hemmes, P. and S. Petrucci, J. Phys. Chem., 72, 3986 (1968).
71. Katzin, L. I., Transition Metal Chem., 3, 56 (1966).
72. Cotton, F. A. and G. Wilkinson, "Advanced Inorganic Chemistry," Interscience Publishers, 1962.
73. Marianelli, R., Ph.D. Thesis, University of California, Berkeley, California, 1966.
74. Reuben, J. and D. Fiat, Chem. Commun., 729 (1967).
75. Choppin, G. R. and A. Graffeo, Inorg. Chem., 4, 1254 (1965).
76. Spedding, F. H. and S. Jaffe, J. Amer. Chem. Soc., 76, 884 (1954).
77. Spedding, F. H., M. J. Pikal, and B. O. Ayers, J. Phys. Chem., 70, 2440 (1966).

78. Hoard, J. L., B. Lee and M. D. Lind, J. Amer. Chem. Soc., 87, 1612 (1965).
79. Nancollas, G. H. and N. Sutin, Inorg. Chem., 3, 360 (1964).